Università degli Studi di Padova

Dipartimento dei Beni Culturali:
Archeologia, Storia dell'Arte, del Cinema e della Musica

Laurea Magistrale in SCIENZE ARCHEOLOGICHE

Curriculum in
APPLIED SCIENCES TO
CULTURAL HERITAGE MATERIALS AND SITES

"Archaeological and technical analysis of Byzantine textile fragments from the site of Zeytinli Bahçe"

Supervisor

Prof. Margarita Gleba

Master Candidate

Ned M. Niko Gelfars

This page is intentionally left blank

Table of Contents

This page is intentionally left blank

Acknowledgements

It is customary to preface a work such as this by extending thanks to those individuals who have either guided or assisted the author in the pursuit of their scholarly goals. Here let it not be ascribed to mere custom, but rather to great affection and the utmost sincerity, that the author expresses their profound gratitude to the following: Professor Margarita Gleba, undisputed authority on all things textile, without whom the present work would scarcely exist as a gleam in the eye of the tutelary genius of the academy; Professors Marcella Frangipane and Francesca Balossi Restelli, of the University of Rome '*La Sapienza*', whose work at Zeytinli Bahçe laid the foundations of the present study, and who graciously provided access to the textile samples investigated herein; Dr. Federico Zorzi, of the CEASC, who suffered the author to try, fail, and ultimately approach success in the task of obtaining useful SEM imagery, and who was almost entirely responsible for the EDS analysis presented in this work; Dr. David Vicenzutto of the University of Padova's *Dipartimento di beni culturali*, who provided access to UniPD's *Laboratori di Archeologia*; and Dr. Emanula Faresin, of that same institution, whose photographic skills permitted the inclusion of numerous illustrations herein; Dr. Caroline Vogt, of the *Abegg-Stiftung*, who was solicitous enough to assist me in the ultimately fruitless task of finding artefacts comparable with the pieces under discussion here; and finally, Penelope Margeotes, as much a weaver as her namesake — and, incidentally, the author's mother.

Τῆς παιδείας ἔφη τὰς μὲν ῥίζας εἶναι πικράς, τὸν δὲ καρπὸν γλυκύν.

Diogenes Laertius, *Lives of the Eminent Philosophers*, 5.1.18

Abstract

In the following thesis are presented the results of a multidisciplinary investigation into a collection of 26 textile fragments discovered in a mediaeval Christian cemetery at the site of Zeytinli Bahçe, in southeastern Turkey. The aim of this investigation was twofold: to characterize the structural parameters, material composition, and conservation status of these fragments; and further, to situate these artefacts within a broader archaeological, historical context. In pursuance of these aims, the author advanced a suite of analytic techniques: autoptic observation coupled with digital microphotography, for quantitative and qualitative analysis of the fragments; scanning electron microscopy (SEM), to obtain high-resolution imagery of the fragments' surface morphology; energy-dispersive x-ray spectroscopy (EDS/EDX), to characterize the elemental composition of the surfaces of the fragments; and finally, radiocarbon dating, to approximate the age of the artefacts. Through the careful application of these techniques, it was determined that the textile fragments are balanced tabbies of variable thread count, composed of z-twisted cotton threads of variable diameter. It was further determined that the fragments are highly deteriorated, with evidence of long-term physical and chemical degradation — including the presence of possible copper corrosion products.

The present work represents the first comprehensive study of the textile fragments found in the mediaeval layers of Zeytinli Bahçe. It serves further as a demonstration of the value of a multidisciplinary approach — integrating technical, archaeometric analyses and conventional archaeological methods — for the study of archaeological textiles.

Riassunto in Italiano

Il presente elaborato illustra i risultati delle analisi archeologiche e tecnico-scientifiche condotte su una collezione di tessuti di epoca bizantina medievale, rinvenuti presso il sito di Zeytinli Bahçe, nell'attuale territorio della Turchia. Scopo principale della ricerca è l'identificazione e la caratterizzazione dei frammenti tessili e dei materiali costitutivi, nonché la loro contestualizzazione in un quadro storico e archeologico più ampio. A tal fine, sono state impiegate diversi metodi analitici, tra cui osservazione autoptica, microfotografia digitale, microscopia elettronica a scansione (SEM) e spettroscopia EDS (energy-dispersive X-ray spectroscopy). È stata inoltre eseguita una datazione al radiocarbonio al fine di determinare l'età approssimativa del corpus analizzato. Il presente studio rappresenta la prima indagine sistematica e approfondita sui frammenti tessili provenienti dagli strati medievali di Zeytinli Bahçe e costituisce un esempio emblematico dell'efficacia di un approccio multidisciplinare, che integra metodologie analitiche, tecniche archeometriche e pratiche archeologiche convenzionali, nello studio dei materiali tessili di interesse archeologico.

L'analisi strutturale dei tessuti, condotta mediante osservazione autoptica e microfotografia digitale con sistema Dino-Lite, ha consentito una dettagliata caratterizzazione dei campioni, i quali risultano essere tessuti in armatura a tela equilibrata, con densità di fili e diametro variabile, realizzati con filati ritorti in senso orario (a 'z'). Tale analisi ha inoltre permesso di rilevare ulteriori elementi diagnostici, quali tracce di cuciture e potenziali sottoprodotti della degradazione.

Le indagini mediante SEM hanno prodotto immagini ad alta risoluzione della morfologia superficiale dei frammenti, rendendo possibile l'identificazione delle fibre come cotone. Al SEM, tali fibre presentano una morfologia distintiva, appiattita e nastriforme, con torsioni longitudinali caratteristiche. Le immagini ottenute documentano in modo evidente tali tratti morfologici, osservabili in tutti i campioni esaminati. Il SEM ha inoltre rilevato segni evidenti di deterioramento, tra cui deformazioni, rotture delle fibre e la presenza di materiali esogeni.

L'applicazione della spettroscopia EDS ha integrato i risultati del SEM, fornendo informazioni sulla composizione elementare delle superfici dei campioni. Gli spettri acquisiti indicano chiaramente la presenza di rame e altri elementi, offrendo dati significativi sui processi di alterazione post-deposizionale che hanno interessato i frammenti, e suggerendo un probabile contatto con altri manufatti metallici al momento della deposizione.

Il capitolo conclusivo analizza il significato complessivo dei risultati ottenuti, sia nel contesto specifico dell'archeologia di Zeytinli Bahçe, sia in relazione alla cultura materiale del periodo bizantino medievale nel suo complesso.

I. Introduction

Zeytinli Bahçe Höyük (Turkish: 'The Mound of Zeytinli Bahçe') is located on the eastern bank of the Euphrates, just south of the modern city of Birecik, Turkey (see **Figure 1**). The site occupies a strategic position along the river — which has served as a natural border between east and west since antiquity — and its history stretches back unto the Chalcolithic. The earliest settlements at Zeytinli Bahçe are dated to the late 4th and early 3rd millennia B.C, coinciding with what is termed the Late Uruk, which period saw the expansion of complex urbanised societies in Mesopotamia and the surrounding region; indeed, the upper Euphrates likely marked the northernmost limit of Uruk influence (Frangipane et al. 2004; Nissen, Lutzeier, and Northcott 1988). After what appears to have been a long and relatively stable period of habitation, the prehistoric settlements at Zeytinli Bahçe were destroyed and subsequently abandoned by the end of the Middle Bronze Age, circa the 2nd millennium B.C (Frangipane et al. 2011). By the first century A.D., the site served as an outpost on the eastern Roman *limes*; the Roman encampment stood in close proximity to the frontier city of Zeugma, where was located one of the most significant river crossings on the Euphrates (Alvaro, Balossi, and Vroom 2004; Pollard 2000). Archaeological evidence suggests that the site continued to function as a fortified outpost or 'castle' during the Byzantine period (Frangipane et al. 2004, p.36). Following the Umayyad military campaigns of the 7th century, the broader region, and perhaps Zeytinli Bahçe itself,

Figure 1: Geographical position of Zeytinli Bahçe and neighbouring Byzantine sites (after Dell'Era 2012).

experienced a period of sociopolitical instability and a concurrent decline in population levels (Alvaro, Balossi, and Vroom 2004; Decker 2007). Subsequent religious crusades and military intrigues effected further instability, with evidence of both Christian and Islamic occupation at the site, and it was not until the 12th century that the area returned to full Byzantine control. (Alvaro, Balossi, and Vroom 2004; Frangipane et al. 2011).

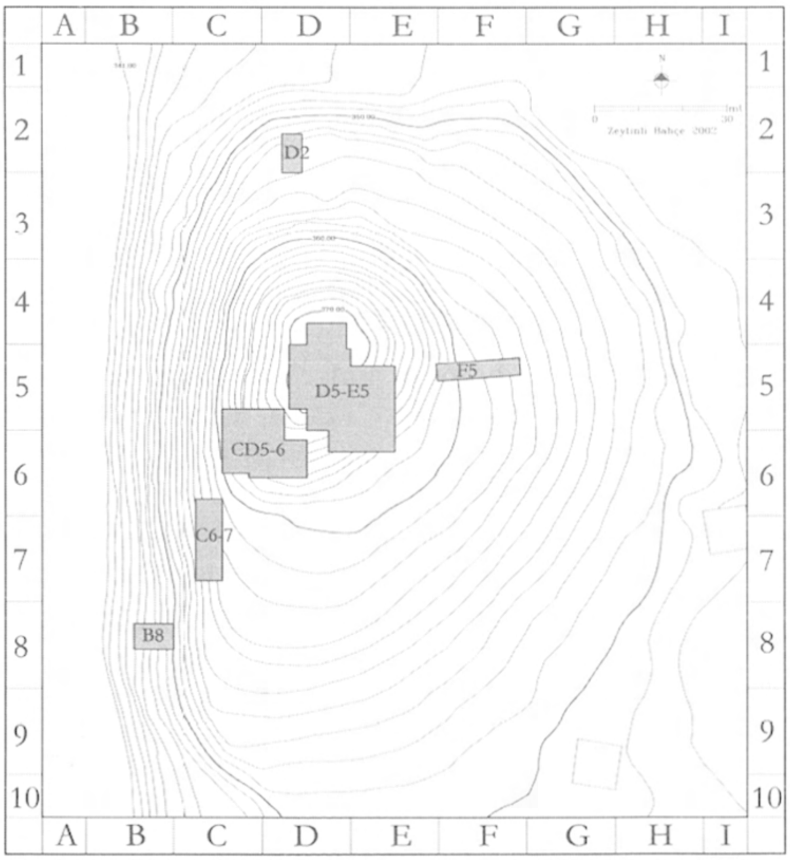

Figure 2: Topography of Zeytinli Bahçe and location of excavation trenches following the 2002 campaign (after Dell'Era 2012).

The present-day archaeological site of Zeytinli Bahçe comprises a large mound, spanning 2.6 hectares and rising approximately 30 meters above the surrounding alluvial plain. The mound is characterized by two distinct tiers: a flat, broad lower mound oriented north-to-south, measuring 16 meters high; and a second mound — the 'central cone' — measuring 50 meters in diameter and 10 meters high (see **Figure 2**) (Dell'Era 2012). The western slope of the mound abuts the Euphrates; it has therefore been subject to significant fluvial erosion, resulting in a steep grade. The central cone is steep on all sides; this fact has been interpreted as a 'structural inconsistency' between the central cone and the lower mound, and has led excavators to hypothesize that the former is artificial rather than sedimentary in origin (Frangipane et al. 2004, p.42).

In anticipation of the construction of the Karkemish Dam, salvage excavations were undertaken at Zeytinli Bahçe beginning in 1999. The excavations were carried out by a team from the University of Rome '*La Sapienza*', under the direction of Professor Marcella Frangipane, and with the cooperation of the Urfa Museum and the permission of the Turkish Ministry of Culture and Tourism. Due to the size of the mound and the poor conditions on its western slope, excavations have proceeded in a strategic fashion, with the aim of piecing together the chronology of Zeytinli Bahçe rather than excavating the site in its entirety (Frangipane et al. 2004). Research has therefore been concentrated on the central cone; the south/south-western slope; and, to a limited extent, the northern and eastern part of the lower mound (see **Figure 2**) (Dell'Era 2012).

Between 1999 to 2002, excavators uncovered a complex stratigraphical sequence at the site, demonstrating a nearly continuous occupation from the 4th millennium B.C. unto the mediaeval period. The sequence consists of superimposed Chalcolithic, Bronze Age, Iron Age, Roman, Early Byzantine, Islamic, and mediaeval (Middle-Late Byzantine) phases (Alvaro, Balossi, and Vroom 2004; Frangipane et al. 2004; 2011). Reconstructing the chronology of the site has proved difficult; the layers are characterized by extensive reconstruction, and the apparent repurposing of pre-existing structures; moreover, erosion on the western slope of the mound seems to have resulted in disruptions to the original sequence, and the loss of objects of potentially diagnostic significance. Consequently, a comprehensive stratigraphy of the site has yet to be advanced (Alvaro, Balossi, and Vroom 2004). Much of the admittedly scant scholarly literature concerning Zeytinli Bahçe deals with the earliest, prehistoric phases of the site. Fortunately for the purposes of the current study, the most recent stratigraphical layers — that is, the mediaeval layers — and the artefacts associated therewith have been documented at some length, chiefly by Dell'Era (2012), to whom many thanks are due.

The mediaeval sequence is limited mainly to the central cone, and has been subdivided into four distinct layers. The earliest layer ('Phase 4') consists of individual 'modular' buildings enclosed within a massive mudbrick wall, and has been interpreted as a fortified outpost or barracks; radiocarbon dating of carbonised wooden fragments retrieved from this layer has provided a date between the 9th and 10th centuries A.D. (Alvaro, Balossi, and Vroom 2004; Dell'Era 2012; Frangipane, Di Nocera, and Siracusano 2011). The second layer ('Phase 3') consists of a single building constructed within the confines of the earlier wall, and has likewise been interpreted as a fortified military structure, albeit a larger and more permanent one (Alvaro, Balossi, and Vroom 2004). The third layer ('Phase 2') represents the final period of occupation and is constituted by a courtyard surrounded by small domestic buildings (Alvaro, Balossi, and Vroom 2004). The topmost layer of the mediaeval sequence consists of a cemetery, containing over forty graves cut into the previous layers. The discovery of six metal crosses in one of these graves testifies to the assumption that the cemetery belonged to a Christian settlement (Dell'Era 2012).

Figure 3: Fragments discovered in connection with beads of uncertain composition, likely bronze. Images courtesy of M. Fragipane.

Figure 4: A textile fragment found in connection with a semi-precious bead (after Dell'Era 2012).

Excavations of the mediaeval sequence have yielded an impressive number of artefacts, including weaponry; religious objects; jewellery; domestic objects; and grave goods (Dell'Era 2012). The latter category of objects includes numerous textile fragments. Some of these fragments were found in connection with — and in some cases directly affixed to — other artefacts, including stone beads of variable composition; and, in at least one case, a ring (see **Figure 3**) (Dell'Era 2012). In one of the graves, a semi-precious stone was found attached to a textile fragment which has been tentatively interpreted as the remains of a bag or purse; this piece also exhibits what appears to be a seam (see

Figure 4) (Dell'Era 2012). Three of these fragments exhibit a greenish residue, which is plainly visible in the images provided.

Figure 5: A partial selection of the full number of fragments, after repackaging by the author. Photo by E. Faresin.

In addition to the pieces just mentioned, more than two dozen textile fragments were uncovered in the cemetery on the central cone during the 2005 campaign (see **Figure 5**). The excavation reports do not provide a description of the context or contexts in which the fragments were found; indeed, precious little information concerning this collection — or, for that matter, any of the textiles, textile tools, or related artefacts discovered at Zeytinli Bahçe — is available. The present work aims to investigate the structural parameters, composition, conservation status, and archaeological significance of these pieces; as far as the author is aware, it represents the first attempt to study the collection at any length.

II. Samples

The collection of textile fragments consists of 26 individual pieces, all of which were excavated from the topmost layer of Zeytinli Bahçe during the 2005 campaign. From the very first preparatory, taxonomical exercises, these textiles proved a daunting object of study. In August 2024, the pieces were received by the author in the packaging prepared by the original excavators. The fragments were labelled 'E7', 'E8', or some combination of the two; these labels correspond to the precise area in the excavation grid in which they were found (see **Figure 2**). The fragments were further labelled by burial number (indicated by 'S' ['*sepoltura*']) and buried individual (indicated by 'H' ['*homo*']). For the purposes of clarity, and given that all of the textiles were excavated in the same area of the grid, the individual pieces in the collection are hereafter categorized using only these latter two elements. The collection, therefore, is divided into five assemblages: S185H268 (consisting of 2 fragments); S192H275 (2 fragments); S196H282 (16 fragments, subdivided into 3 groups [Y1; Y2; and Y2L]); S208H305 (2 fragments, subdivided into 2 groups [Y1; and Y2]) and S211H310 (4 fragments, subdivided into 3 groups [Y1; Y2; and Y3]) (see **Figure 6** for an illustration of these admittedly bewildering divisions and subdivisions).

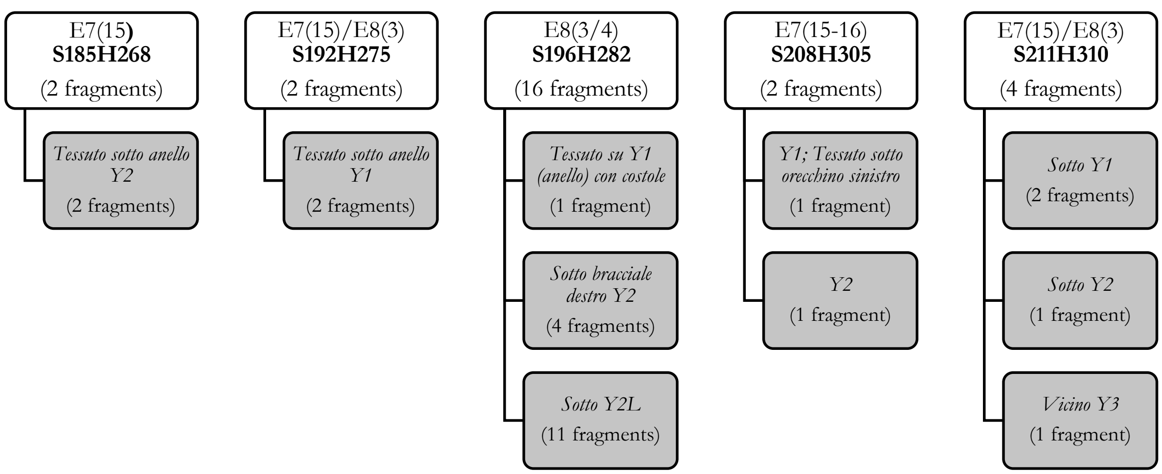

Figure 6: Chart illustrating the categorization of the 26 textile fragments. The collection is divided into 5 distinct assemblages, each corresponding to a particular burial and buried individual; these assemblages are further subdivided by the descriptions provided by the excavators.

To the best of the author's knowledge, no description of these fragments, nor the precise location or conditions in which they were deposited, has yet been offered in any of the excavation reports. Be that as it may, the excavators' subdivision of the fragment assemblages into different groups appears to correspond to the location either within the grave or the broader funerary area where the fragments in question were found. The 2 fragments associated with S185H268 are labelled '*Tessuto sotto anello Y2*' ('Textile under ring Y2'). The 2 fragments associated with S192H275 are labelled '*Tessuto sotto anello Y1*' ('Textile under ring Y1'). The 16 fragments associated with S196H282 are subdivided in 3: 1 fragment is labelled '*Tessuto su Y1' (anello) con costole* ('Textile on Y1 [ring] with rib'); 4 fragments are labelled '*Sotto bracciale destro Y2*' ('Under right bracelet Y2'); and 11 fragments are labelled '*Sotto Y2L*' ('Under Y2L'). The 2 fragments associated with S208H305 are labelled '*Y1*' and '*Y2*', respectively; the first of these, S208H305 Y1, is further labelled '*Tessuto sotto orecchino sinistro*' ('Textile under left earring'). Finally, the 4 fragments associated with S211H310 are subdivided in 3: 2 fragments are labelled '*Sotto Y1*' ('Under Y1'); 1 fragment is labelled '*Sotto Y2*' ('Under Y2'); and 1 fragment is labelled '*Vicino Y3*' ('Near Y3'). Some of these labels are unambiguous; the author presumes, for example, that those fragments labelled '*sotto orecchino sinistro*' were so designated due to their being found under the right earring of one of the buried individuals. However, it will suffice to say that most of these labels are decidedly unclear. It is likely that '*anello*' refers to a literal ring, rather than a specific area of the excavation; however, the references to 'Y1', 'Y2', *et cetera*, are inscrutable.

Figure 7: S196H282 Y2L Fragment 6. Photo by E. Faresin.

Figure 8: S192H275 Fragment 1. Photo by E. Faresin.

After sorting, the collection was documented and photographed by the author on the premises of the University of Padova's *Laboratori di Archeologia*, in Ponte di Brenta. The fragments were then carefully repackaged in plastic find bags so as to ensure their preservation. Further photography was later undertaken by Dr. Emanuela Faresin at the *Laboratori di Archeologia*. For a full catalogue of the textiles, with accompanying photographs, see **Appendix**.

Textiles represent some of the rarest archaeological finds; like other organic materials, they are subject to rapid post-depositional deterioration by chemical, physical, and microbial agents, and are typically preserved only in specific environmental conditions. To make matters even more difficult, the degradation of archaeological textiles is often furthered by handling -– a fact to which the author can readily testify (Gleba and Mannering 2012; Gillis and Nosch 2007). The conservation status of the textile fragments under examination here is generally poor; several pieces have deteriorated nearly to the point of disintegration; others consist of only a few threads (see **Figure 7**) or indeed individual fibres. Moreover, due to their never having been subject to any sort of conservation, many of the pieces are encrusted in soil (see **Figure 8**). For these reasons, analysis of the fragments posed a significant challenge. Notably, the 2 fragments associated with S208H305, and 2 of the fragments associated with S211H310, are in such poor condition as to elude analysis altogether; indeed, so minute are these pieces that autoptic observation alone was insufficient for determining whether they were indeed fibres, as opposed to soil or some other exogenous material.

III. Analysis – methods

Each textile fragment in the collection was subject to autoptic observation and microphotography using a Dino-Lite digital microscope set at various magnifications; these observations were supplemented with scanning electron microscopy (SEM), and energy-dispersive x-ray spectroscopy (EDS/EDX). In order to preserve the textile fragments, only a small number of the full collection was sampled and subject to the latter two techniques. Finally, one fragment was sent to the *Koninklijk Instituut voor het Kunstpatrimonium - Institut Royal du Patrimoine Artistique* (KIK-IRPA), in Brussels, for radiocarbon dating.

III.1. Textile structural analysis

The aim of textile analysis is to characterize the structural parameters of the pieces under investigation, and of the individual threads of which they are composed (Gleba 2017b). These parameters include: **weave type**; **thread diameter**; **thread count**; and **thread twist** (Emery 1995). Individually and in combination, these parameters may serve as cultural and/or chronological indicators; the significance of each parameter is detailed in the following subsections. Besides structural characterization, textile analysis permits the identification of diagnostic features such as edges and decorations (Gleba 2017b). Textile analysis was carried out by the author over the course of several weeks, via autoptic observation and digital microphotography using a Dino-Lite AM7115MZT digital microscope. In effect, the Dino-Lite functions as a simple optical microscope; a built-in LED light source illuminates the sample surface, and the resultant image is transmitted onto a computer monitor using the proprietary Dino-Lite software, DinoXcope (Gigilashvili, Lukesova, and Hardeberg 2024). Digital microphotography was undertaken at set magnifications (20x, 50x, and 220x); the parameters listed above were then ascertained via observation, or quantified using the manual measurement function included in the DinoXcope software.

III.1.a. Weave type

In simple terms, a textile is defined as a fabric composed of two distinct sets of elements — typically threads derived from plant or animal fibres, or from other, non-organic sources. These two elements are termed the warp, that is, a set of parallel threads held under tension longitudinally on the loom; and the weft (or woof), that is, a set of parallel threads interworked with the warp, generally at transverse angles (Barber 1991; Emery 1995). The interworking of these sets of threads is what is more commonly known as weaving, and may be carried out in numerous ways; the manner in which the sets are interworked in a given textile is known as the weave. Simple weaves are those which contain only one set of longitudinal elements, and only one set of transverse elements (Emery 1995). Of the simple weaves, the very simplest is the plain or tabby weave; in plain-woven textiles, the individual weft units pass under and over the individual warp units in 'unvarying alternation' (see **Figure 9**) (Emery 1995, p.76). Perhaps due to the simplicity of their construction, tabbies likely represent some of the earliest documented loom-woven fabrics (Barber 1991; Gleba 2017b). Plain-woven textiles may be further subdivided into various types, including: balanced plain weave, wherein the warp and weft are of comparable if not identical size and distribution; warp-faced plain weave, wherein the warp threads outnumber the weft threads by at least two to one, thereby concealing them; and weft-faced plain weave, the reverse of the foregoing, that is, wherein the weft threads outnumber the warp threads by the same margin, thereby concealing them (Barber 1991; Emery 1995; Gleba 2017b).

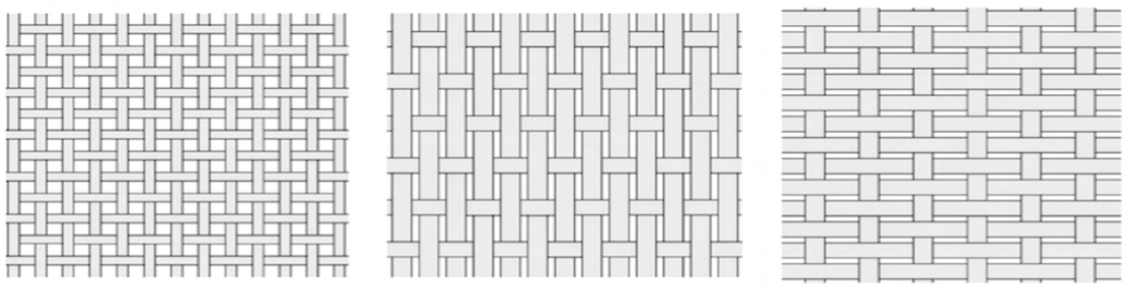

Figure 9: (Left to right) balanced plain weave; warp-faced plain weave; weft-faced plain weave (after Gleba 2017a).

III.1.b. Thread count

Thread count refers to the quantity of warp and weft threads per linear unit of measurement — in this case, per centimetre (Emery 1995). Thread count is a qualitative as well as a quantitative measure. Insofar as fine fabrics typically exhibit a higher thread count than do coarse fabrics, measurement of thread count can serve as means of determining the quality of archaeological textiles; it can moreover provide information on the tools and techniques used to manufacture particular fabrics (Hammarlund 2005).

III.1.c. Thread diameter

A relatively uncomplicated parameter to be measured in the course of textile analysis, thread diameter refers to the diameter of the individual threads composing the warp and weft (Emery 1995). Measurements of thread diameter was facilitated by using the manual measurement function included in DinoXcope.

III.1.d. Thread twist

In preparation for the process of weaving, natural fibres must be transformed into workable thread. Organic fibres such as wool and cotton are quite short and fragile, and so must be twisted together into a continuous strand suitable for weaving (Emery 1995). The act of twisting together these fibres is termed spinning; archaeological evidence suggests that the earliest use of spinning technology dates to the Palaeolithic (Barber 1991; Gleba and Mannering 2012). Characterization of thread twist entails the description of two parameters: thread twist direction; and tightness or angle of twist. During the process of spinning, threads can be twisted in one of two directions; threads are described as z-twisted (notated 'z') if spun clockwise, and s-twisted (notated 's') if spun counter-clockwise; those threads exhibiting no discernible twist are notated 'i' (see **Figure 10**) (Gleba 2017a). Thread twist can be further characterized by tightness or angle of twist, which can refer to: the angle made by the fibres along the thread's vertical axis; the number of twists exhibited per unit of measurement; or some combination of the two (Emery 1995). Tightness is typically quantified as loose (up to 20°), medium (20-40°) or hard (over 40°), but is sometimes provided as a qualitative approximation (Emery 1995).

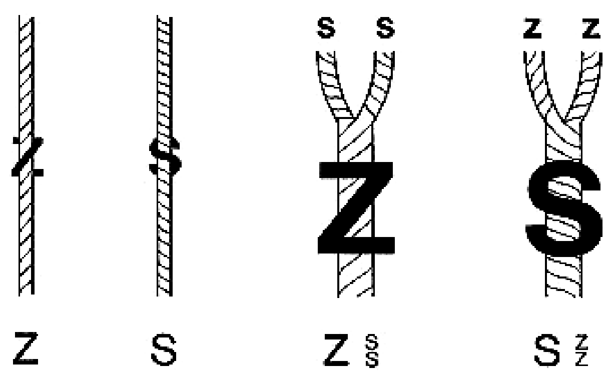

Figure 10: (Left to right) z-twisted and s-twisted threads (after Bender Jørgensen 2004).

III.1.e. Other diagnostic features

In addition to the structural parameters discussed above, textile analysis permits the identification of various diagnostic features. These include ornamentation and decoration, borders edges, sewing elements, and other culturally-relevant elements (Gleba 2020).

III.2. Scanning electron microscopy (SEM)

Scanning electron microscopy (hereafter, SEM) is a high-resolution imaging technique which generates detailed surface topography and microstructural information of a given sample; as compared with conventional light microscopy, SEM has significantly greater magnification (Rezić, Ćurković, and Ujević 2010; HAMM 2014; Markova 2019). SEM images are generated from the interaction between a focused beam of high-energy electrons produced by a thermal emission source, and the atoms constituting the sample surface. As the electron beam hits these atoms, it elicits the emission of characteristic electromagnetic signals therefrom; these signals are detected by the SEM instrumentation, and 'translated' into a high-resolution greyscale image (Ponting 2004; Artioli 2010). The electromagnetic signals used to generate SEM images are of various kinds; the most significant for the purposes of this study are backscattered electrons — that is, high-energy electrons originating from the sample surface by elastic scattering events — and secondary electrons — that is, low-energy electrons originating from the sample surface by inelastic scattering events. (Artioli 2010; HAMM 2014). The SEM column and sample chamber are maintained in a vacuum of variable pressure, which permits the electrons to travel between the sample surface and the detector (HAMM 2014).

The use of SEM for the investigation of archaeological textiles is well-established (Rast-Eicher 2016). The high-resolution imaging capability of SEM enables detailed visualization of textile fibres' surface morphology, facilitating the characterization of structural features and degradation processes. Textile fibres can be analysed via SEM either longitudinally or in cross-section; each method permits the collection of different information vis-à-vis the morphological characteristics of the fibre in question (Markova 2019). Furthermore, SEM is non-invasive; for this reason, it is particularly valuable for the study of archaeological artefacts, insofar as it permits the samples under investigation to be preserved, and thus subjected to further analytic techniques (Coletti et al. 2024). Finally, when used in conjunction with conventional textile analysis, SEM can permit the unambiguous identification of fibre type and species — however, given the poor state of conservation typically associated with archaeological textiles, a positive identification of species requires proficient use of the SEM instrumentation, and expert analysis of the generated images (Artioli 2010). It is typically recommended that archaeological textiles be examined under low-pressure as to opposed to high-pressure vacuum settings, due to the fragility of these sorts of artefacts (Lukesova and Holst 2024).

Perhaps the most significant challenge for researchers conducting SEM on archaeological textiles is that of charging — that is, the generation of anomalous surface imagery, and concurrent loss of image quality, as a result of excess surface charge (Shaffner and Veld 1971). The problem of charging is a major concern for the analysis of textiles given their fragile nature, and their non-conductivity. This problem can be mitigated by the application of a microscopic layer of conductive material prior to

SEM analysis; typically, a gold or carbon coating is used, but platinum-palladium has also proven advantageous for the analysis of archaeological textiles (Suomela et al. 2023; Lukesova and Holst 2024).

In the context of the present study, the aim of SEM was twofold: one, the identification of fibre type; and two, the characterization of any microscopic evidence of degradation. SEM was conducted on the premises of the *Centro di Analisi e Servizi Per la Certificazione* (CEASC), at the University of Padova, using a COXEM EM-30AX Plus tabletop SEM equipped with a tungsten filament for the generation of the electron beam (see **Figure 11**). Ten samples were selected from the collection of textile fragments; at least 1 sample from each assemblage was chosen, with the exception of S208H305, which was determined to consist only of exogenous materials. Millimetre-sized (or smaller) samples of the fragments to be analysed were affixed onto aluminium mounting stubs with adhesive carbon tape (see **Figure 12**). The fragments were left uncoated in order to preserve them for further analysis. SEM images were then generated at various magnifications (100-1000x) using both backscattered and secondary electrons, with the SEM column and sample chamber set to a low-pressure vacuum, and accelerating voltage set between 15 and 20 kV. Following the generation of these images, longitudinal characteristics of the samples were observed and analysed with reference to their morphology.

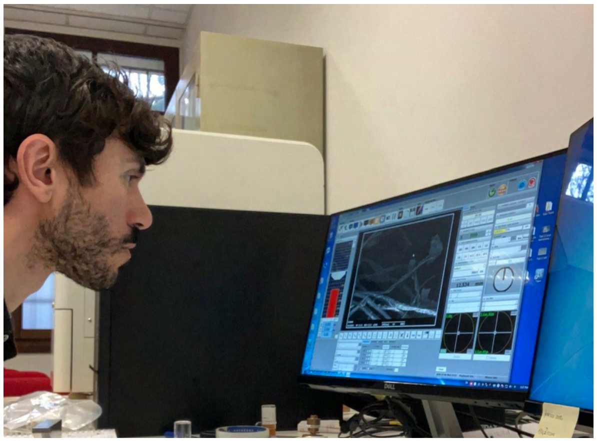

Figure 11: The author engaged in SEM analysis on the premises of the CEASC. Photo by the author.

Figure 12: 3 of the textile fragments, affixed with adhesive tape on aluminium mounting stubs. Photo by E. Faresin.

III.3. Energy-dispersive x-ray spectroscopy (EDS)

Energy-dispersive x-ray spectroscopy (otherwise known as EDS or EDX; hereafter referred to as EDS) is a form of x-ray fluorescence spectroscopy; used in combination with SEM, it collects and analyses the characteristic x-rays generated by the interaction between an electron beam and a given sample surface (Artioli 2010). The EDS detector — typically a lithium-drifted silicon, solid-state device — measures the relative abundance of the emitted x-rays versus their respective intensities; after gathering these data, the EDS software generates a spectrum illustrating the particular elements present within the sample, as well as the relative concentration percentages thereof (HAMM 2014; Dickey 2022). EDS also permits the generation of elemental maps of a given sample, by measuring x-ray intensity relative to lateral position on the sample surface (Artioli 2010; HAMM 2014).

As with SEM, the use of EDS for the analysis of archaeological artefacts is well-established — if less frequently applied (Dickey 2022). Properly carried out, and with appropriate interpretation of the resultant data, EDS permits the characterization of material composition and degradation processes, and the detailed visualization of the surface morphology and topology of the sample in question. Like SEM, it is a non-destructive technique, and is therefore suitable for the analysis of archaeological textiles. Indeed, since the 1980s, EDS has been increasingly used for the quantitative and qualitative analysis of both plant and animal fibres; it has proven particularly useful for the identification of degradation products, and the characterization of mineralized textile fragments (Rezić, Ćurković, and Ujević 2010; Dickey 2022).

There are two notable drawbacks to the application of EDS in the context of an investigation such as this. The first is that EDS is limited to investigating the surface of the sample — that is, the electrons generated during the procedure are capable of penetrating only several micrometres of material (Rezić,

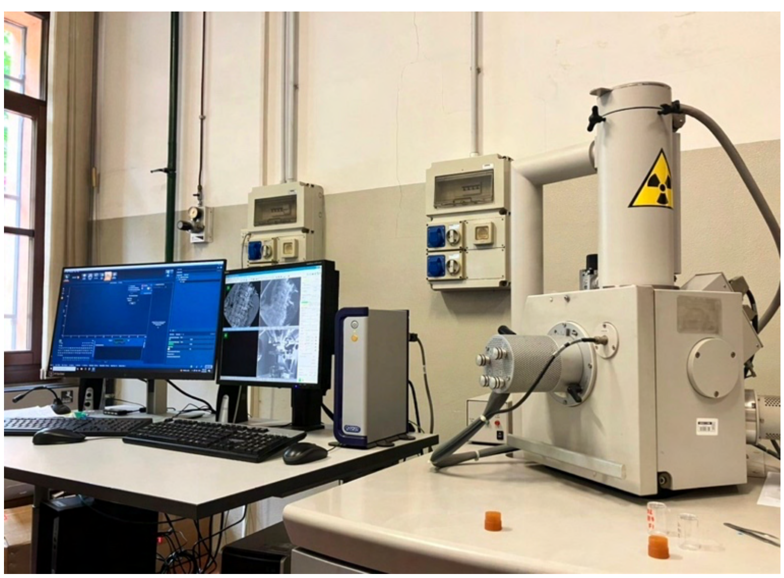

Figure 13: FEI Quanta 200 ESEM with computer running AZtecTEM software on the premises of CEASC. Photo by the author.

Ćurković, and Ujević 2010). Thus, EDS is insufficient for the comprehensive characterization of the composition of archaeological artefacts, textiles or otherwise. The second major problem is that of contamination, either by post-depositional processes or by improper handling; even trace quantities of contaminants can render EDS data useless (Dickey 2022).

SEM-EDS was conducted at CEASC on 23 April 2025, under the supervision of Dr. Federico Zorzi, using an FEI Quanta 200 Environmental Scanning Electron Microscope (ESEM) in combination with an Oxford Xplore 30 EDS detector; AZtecTEM software was then used for data analysis and generation of spectra and elemental maps (see **Figure 13**). Due to time constraints, only two of the samples previously subject to SEM were analysed by means of SEM-EDS: S192H275 Fragment 1; and S211H310 Y2. These samples were chosen due to the visible presence of greenish deposits or residues, as ascertained via autoptic observation and Dino-Lite digital microphotography. The primary aim of the EDS procedure for the purposes of this study was to identify the content of these residues. Following this procedure, the EDS software was used to generate spectra and elemental maps detailing the elemental composition of the textile fragments under investigation.

III.4. Radiocarbon dating

Radiocarbon dating — otherwise known as carbon-14 or ^{14}C dating — is an isotopic dating method by which the age of organic (that is, carbon-based) materials can be approximated; it is effective for materials up to 50-60,000 years old (Artioli 2010). The technique permits the calculation of the approximate age of a given material by measuring the quantity of ^{14}C, a radioactive isotope of carbon, present therein (Margariti et al. 2023). ^{14}C is generated within Earth's atmosphere through the interaction of cosmic rays with atmospheric ^{14}N (nitrogen-14); it subsequently combines with atmospheric oxygen and is converted into carbon dioxide, whereupon it is incorporated into the biosphere through photosynthesis by green plants (Bronk Ramsey 2008; Margariti et al. 2023). ^{14}C is constantly produced in the atmosphere, and thus constantly replenished within the cells of photosynthetic plants, unto their death — by harvesting, pruning, snipping, *et cetera*, in the case of plant fibres; or by shearing, cutting, skinning, *et cetera*, in the case of animal fibres. ^{14}C decays at a constant rate; it follows that by measuring the quantity of ^{14}C in a given organism or remnant thereof, the approximate date of death of said organism can be calculated (Artioli 2010; Margariti et al. 2023).

After sampling, radiocarbon dating proceeds by the application of either decay counting methods, which measure the activity of radioactive carbon atoms within the sample; or accelerator mass spectrometry (AMS), which directly measures the quantity of these atoms (Bronk Ramsey 2008; Artioli

2010). AMS is the preferred method for dating archaeological artefacts, insofar as it requires a relatively small sample — in the case of archaeological textiles, as little as 5 milligrams (Artioli 2010). Put very simply, AMS employs a high-energy ion accelerator in combination with a mass spectrometer to separate atoms and molecules on the basis of their mass-to-charge ratio; this, in turn, permits the quantification of individual isotopes such as ^{14}C (Artioli 2010; Kutschera 2016). Based on the quantity of ^{14}C detected by AMS, a conventional age is calculated; using calibration curves derived from the measurement of the ratio of ^{14}C to C in dendrochronologically-dated tree rings, a calendar date is then acquired (Artioli 2010).

Given that archaeological textiles are typically composed of organic materials — whether animal or vegetable — numerous such artefacts have been subject to radiocarbon dating (Margariti et al. 2023). Indeed, the relatively short 'life span' of organic textiles renders them prime candidates for the technique. Unlike the spectroscopic methods discussed above, however, radiocarbon dating is destructive; samples to be examined therewith must undergo a chemical pre-treatment which concludes with pulverization, and therefore renders them unfit for further analysis (Margariti et al. 2023).

For the purposes of the present study, one sample was selected to undergo radiocarbon dating at the laboratory of the *Koninklijk Instituut voor het Kunstpatrimonium - Institut Royal du Patrimoine Artistique* (KIK-IRPA), in Brussels. KIK-IRPA employs a MICADAS (MIni CArbon Dating System) accelerator mass spectrometer for quantifying the ^{14}C present in the sample. MICADAS is a state-of-the-art, table-top instrument designed specifically for use in radiocarbon dating; it uses a vacuum-insulated acceleration unit operating at an accelerating voltage of 200kV (Synal, Stocker, and Suter 2007; Kutschera 2016).

IV. Analysis – results

IV.1. Textile structural analysis

The structural data acquired via autoptic observation and Dino-Lite digital microphotography are reported in **Figure 14**, and detailed at length in the following subsections. Due to the small size and more or less poor preservation state of the fragments, certain parameters — most significantly, weave and thread count — are tentative. With regard to the fragments associated with S208H305 and S211H310 Y1, scarcely any parameters could be determined; those parameters which could not be determined are designated as 'n/d' in **Figure 14**. Moreover, given that none of the samples is complete, it was not possible for the author to identify warp *contra* weft; consequently, the two systems making up the fragments are listed generically, that is: system 1 and system 2.

Textile	Weave	Sys 1 diam.avg. (mm)	Sys 1 diam.rng. (mm)	Sys 2 diam.avg. (mm)	Sys 2 diam.rng. (mm)	Sys 1 twist	Sys 2 twist	Sys 1 threads counted	Sys 2 threads counted
S185 H268 F1	Plain	0.33	0.22-0.54	0.41	0.32-0.53	z	z	12(6x2)?	14(7x2)?
S185 H268 F2	n/d	n/d	n/d	n/d	n/d	z	z	n/d	n/d
S192 H275 H F1	Plain	0.38	0.22-0.66	0.27	0.16-0.39	z	z	14 (7x2)	22(11x2)
S192 H275 H F2	Plain	0.37	0.19-0.65	0.39	0.17-0.48	z	z	18(9x2)?	20(10x2)?
S196 H282 Y1	Plain	0.44	0.28-0.6	0.49	0.34-0.5	z	z	14(7x2)	16(8x2)
S196 H282 Y2 F1	Plain	0.56	0.36-0.97	0.67	0.48-1.06	z	z	12(6x2)	12(6x2)
S196 H282 Y2 F2	Plain	0.61	0.43-0.99	0.79	0.67-0.96	z	z	10(5x2)?	n/d
S196 H282 Y2 F3	Plain	0.52	0.39-0.71	0.74	0.49-1.29	z	z	12(6x2)	10(5x2)
S196 H282 Y2 F4	Plain	0.45	0.42-0.51	0.42	0.33-0.56	z	z	16(4x4)	16-18(8-9x2)?
S196 H282 Y2 L F1	Plain	0.48	0.36-0.62	0.52	0.34-0.61	z	z	15	14(7x2)
S196 H282 Y2 L F2	Plain	0.51	0.41-0.62	0.53	0.36-0.59	z	z	16(8x2)	16(8x2)
S196 H282 Y2 L F3	Plain	0.45	0.34-0.59	0.36	0.29-0.56	z	z	14(7x2)?	16(8x2)?
S196 H282 Y2 L F4	Plain	0.49	0.35-0.72	0.62	0.49-0.73	z	z	12(6x2)	12(6x2)
S196 H282 Y2 L F5	Plain?	n/d	n/d	n/d	n/d	z	z	8?	n/d
S196 H282 Y2 L F6	Plain?	n/d	n/d	n/d	n/d	z	i?	10(5x2)?	10(5x2)?
S196 H282 Y2 L F7	Plain?	n/d	n/d	n/d	n/d	z	z	n/d	n/d
S196 H282 Y2 L F8	Plain	0.61	0.41-0.89	0.54	0.36-0.76	z	z	12(6x2)?	12(6x2)?
S196 H282 Y2 L F9	n/d	0.51	0.37-0.64	0.66	0.51-0.83	z?	z?	10(5x2)?	12(6x2)?
S196 H282 Y2 L F10	n/d	n/d	n/d	n/d	n/d	n/d	n/d	n/d	n/d
S196 H282 Y2 L F11	n/d	n/d	n/d	n/d	n/d	z?	z?	n/d	n/d
S208 305 Y1	n/d	n/d	n/d	n/d	n/d	n/d	n/d	n/d	n/d
S208 305 Y2	n/d	n/d	n/d	n/d	n/d	n/d	n/d	n/d	n/d
S211 H310 Y1 F1	n/d	n/d	n/d	n/d	n/d	n/d	n/d	n/d	n/d
S211 H310 Y1 F2	n/d	n/d	n/d	n/d	n/d	n/d	n/d	n/d	n/d
S211 H310 Y2	Plain	0.46	0.4-0.62	0.57	0.37-0.72	z	z	10(5x2)	14(7x2)
S211 H310 Y3	Plain	0.56	0.38-0.64	0.44	0.36-0.64	z	z	14(7x2)	16(4x4)

Figure 14: Structural parameters of the textile fragments (weave; average thread diameter of system 1, measured in millimetres; range of thread diameters of system 1, measured in millimetres; average thread diameter of system 2, measured in millimetres; range of thread diameters of system 2, measured in millimetres; system 1 thread twist direction; system 2 thread twist direction; thread count per centimetre of system 1; thread count per centimetre of system 2). Those parameters which could not be determined are marked 'n/d'.

IV.1.a. Weave type

With only a few exceptions, the textile fragments were identified as balanced tabbies (see **Figure 15** for several examples). Those fragments which were not so identified are very badly degraded; that is to say, it was impossible to identify any type of weave. In the case of S196H282 Y2L Fragment 6, for example, the fragment is almost entirely encrusted with conservation product; only a single thread is visible (see **Figure 7**). In this and further instances, therefore, weave identification was unfeasible, as is indicated in **Figure 14**. For other pieces — generally, but not only, larger pieces — identification of weave type was uncomplicated, and indeed possible by autoptic observation alone.

Figure 15: (Left to right) Dino-Lite images of S185H268 Fragment 1; S192H275 Fragment 2; S211H310 Y2 at 50x magnification. All are balanced tabbies.

IV.1.b. Thread count

Given that the majority of the fragments under examination here are scarcely more than a centimetre in length or width, in most cases it was only possible to determine the thread count per half-centimetre; calculation of the thread count per centimetre is therefore expressed as (thread count per half-centimetre x 2). It follows that the measurements reported for the entire collection are approximate.

As is reported in **Figures 14** and **15**, several of the fragments exhibit identical thread counts in both constituent systems, while others exhibit substantial variation between the two systems. The latter observation would seem to testify to the variable quality of the textiles within the collection. However, the range in thread counts between textiles found in the same grave -– notably, S196H282 — suggests that this disparity is the consequence of post-depositional degradation rather than the inherent quality of the textiles themselves. Indeed, as is indicated in **Figure 15**, the thread counts for systems 1 and 2 were relatively consistent across the collection of fragments. **Figure 16** presents a scatter plot detailing the relationship between thread counts measured in the 2 systems. The values reported for system 1 range from 10 to 18 threads per centimetre, while those reported for system 2 range from 10 to 22 threads per centimetre — a spread which suggests some variability between the two systems. There appears to be a general positive trend, however, indicating that higher thread counts in one system tend to correspond to higher counts in the other.

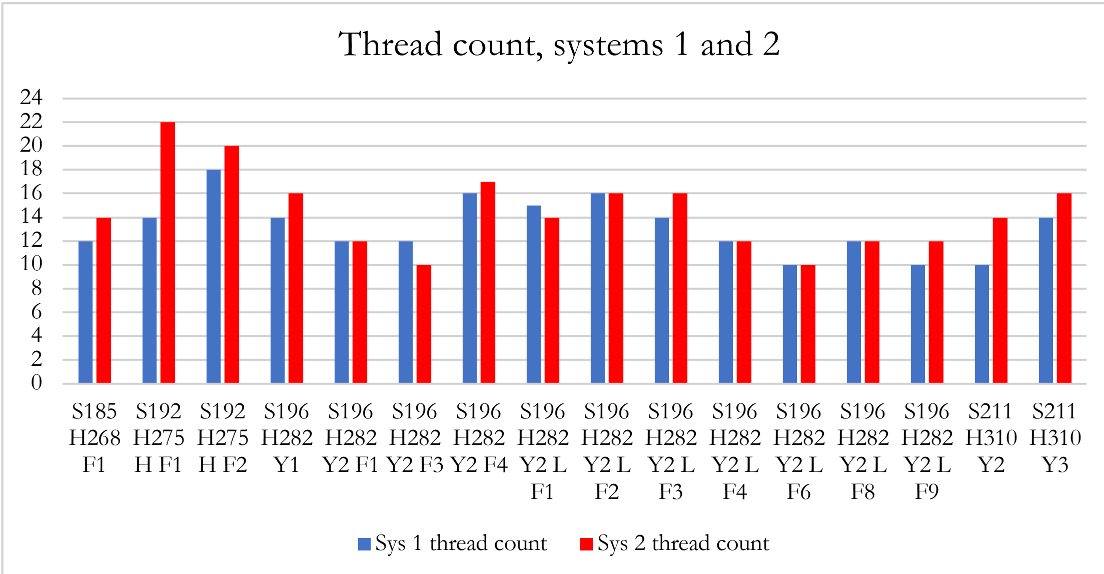

Figure 15: Chart illustrating the thread counts of systems 1 and 2 for each fragment.

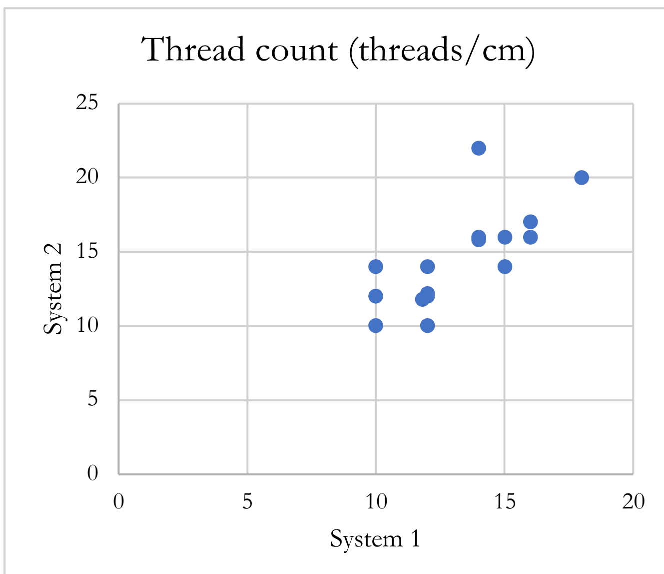

Figure 16: Chart illustrating the distribution of thread counts for systems 1 and 2. Chart by M. Gleba.

IV.1.c. Thread diameter

As is often the case with archaeological textiles, measurement of thread diameter was significantly compromised by the state of conservation of the materials under examination. The threads composing many of the fragments within the collection have become compressed or distorted over time; consequently, the diameter of the constituent threads varies from one area to the next. In the case of

S192H275 Fragment 2, for example, the range of measured diameters in system 1 runs from 0.19 millimetres to 0.65 millimetres, and from 0.17 millimetres to 0.49 millimetres in system 2 (see **Figure 14**). Taking into consideration the entire collection — or rather, those fragments in the collection which it was possible to measure with reasonable accuracy — the measurements are as follows: the diameters of system 1 range from 0.33 millimetres to 0.61 millimetres, while those of system 2 range from 0.27 millimetres to 0.79 millimetres; the average thread diameter of system 1 was calculated at 0.45 millimetres, the average thread diameter of system 2 at 0.50 millimetres. **Figure 17** presents a scatter plot illustrating the average thread diameters of systems 1 and 2. There is a clear positive correlation between the systems; as measurements from system 1 increase, those from system 2 tend to increase as well. Moreover, the data points are closely clustered around a diagonal trend, indicating strong agreement between the two systems with minor variation. Despite the obvious variations between the thread diameters of the individual pieces, these trends suggest a degree of consistency which may not be readily apparent to the casual observer. This may be the consequence of technical skill; homogeneity of the cotton fibres used in producing the textiles; or a combination of the two.

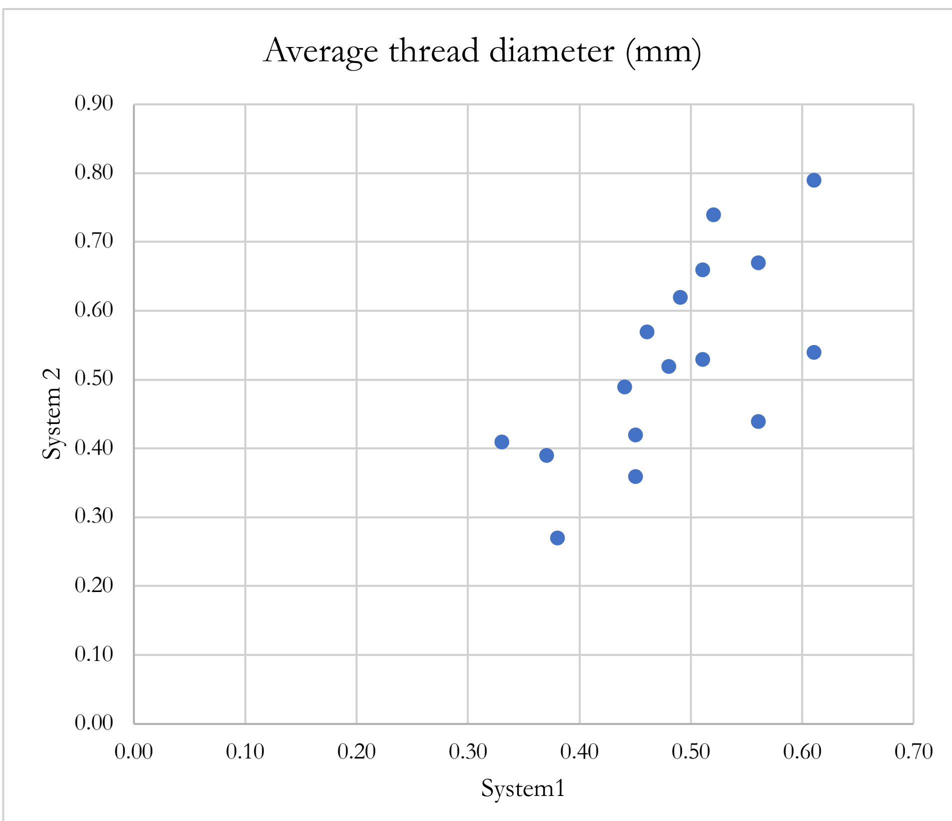

Figure 17: Chart illustrating the distribution of average thread diameters for systems 1 and 2. Chart by M. Gleba.

IV.1.d. Thread twist

Analysis by means of Dino-Lite digital microphotography was sufficient for determining thread twist direction; for almost all of the fragments, the thread was characterized as z-twisted (see **Figure 18**). Thread twist tightness was more difficult to calculate; not only does the thread twist angle vary from one fragment to another, the very threads composing the fragments are more or less tight depending on which region is examined. Given that the threads were hand-spun — and considering, moreover, the poor conservation status of the fragments — this irregularity is unsurprising.

IV.1.e. Other diagnostic features

Not a single fragment within the collection exhibits an identifiable edge; ornamentation, dyeing, and other features are similarly absent. One of the pieces, however, does exhibit what appears to be some sort of seam, which was documented with conventional photography as well as Dino-Lite digital microphotography (see **Figure 19**). As reported in the introduction, a similar feature is present on another textile fragment discovered at Zeytinli Bahçe, but this piece was not analysed in the present study (see **Figure 4**).

The largest piece in the collection is S196H282 Y2 Fragment 1, measuring approximately 9.5 millimetres in length (see **Appendix** for further details). This piece is the closest to intact in the whole collection and is marked by a prominent fold, likely a result of compression rather than a deliberate feature of the textile; the fabric is visibly crushed, the fibres flattened. Indeed, perhaps the most notable feature of many of these pieces is their advanced state of degradation. Many are coated in conservation product, which rendered handling not only difficult but quite messy.

Furthermore, several pieces within the collection exhibit a greenish residue, which is often characteristic of the degradation of copper (see **Figure 20**) (Cronyn 1990). As is the case with the fragments discussed in the introduction, this residue is visible without the aid of microphotography. As is detailed further on in this chapter, EDS analysis confirmed the presence of copper and other elements on the surfaces of the textile fragments.

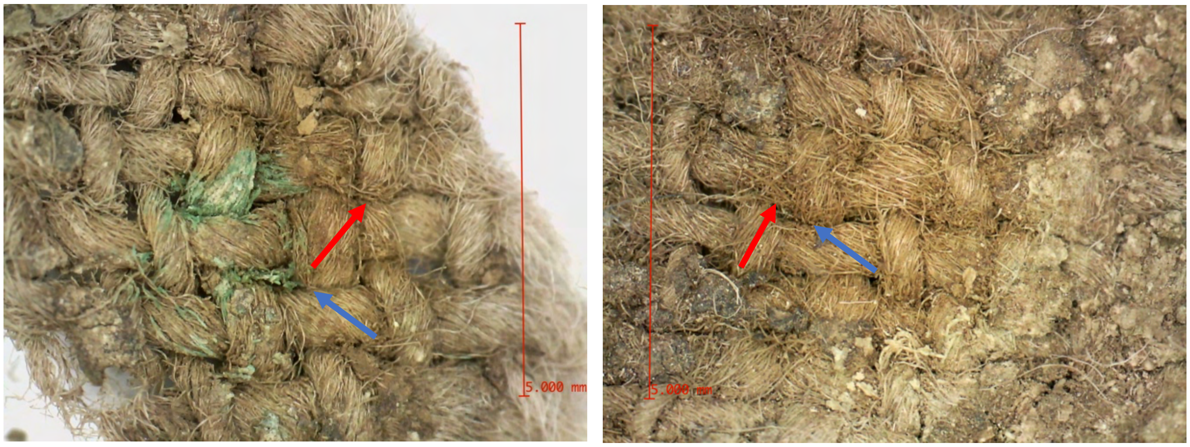

Figure 18: (Left to right) Dino-Lite images of S196H282 Y2L Fragment 4 and Fragment S196H282 Y2 Fragment 1 at 50x magnification. Twist direction of system 1 threads is indicated by the red arrow; twist direction of system 2 threads by the blue arrow.

Figure 19: (Left to right) Dino-Lite images of S196H282 Y1 Fragment 1, at 20x and 50x magnification.

Figure 20: (Left to right) Dino-Lite images of S192H275 Y1 Fragment 1 and S211H310 Y2, both at 50x magnification. Note the greenish residue.

IV.2. Scanning Electron Microscopy (SEM)

Analysis of the images generated via SEM demonstrated unambiguously that all of the samples are composed of cotton. Cotton is a cellulosic fibre derived from the seeds of plants of the genus *Gossypium* (Barber 1991; Markova 2019). As such, it is composed largely of chains of cellulose molecules, aggregated into partially crystallized microfibrils; this fibrous microstructure imparts to cotton its mechanical strength and flexibility (Timar-Balazsy and Eastop 2012; Suomela et al. 2023).

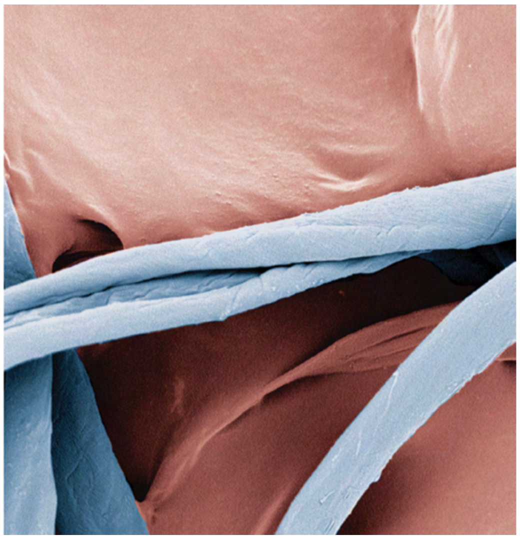

Figure 21: Longitudinal false-colour SEM image of a modern cotton fibre (after Markova 2019).

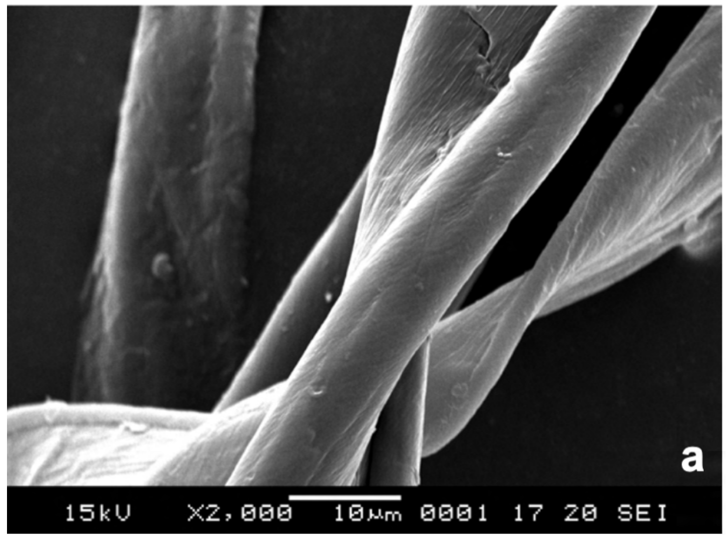

Figure 22: Longitudinal SEM image of a heritage cotton fibre from China (after Cao et al. 2009).

Under SEM, the surface of cotton fibre exhibits a distinctive morphology — that is, a flattened, ribbon-like shape characterized by longitudinal twists, termed convolutions or convolutes (Markova 2019; Lukesova and Holst 2024). These convolutions are the product of the collapse of the fibres' cell walls, following hydration and subsequent air drying (Timar-Balazsy and Eastop 2012). The presence of these characteristic convolutions distinguishes cotton's surface morphology from that of other natural fibres such as flax or wool, and is therefore diagnostic for the identification of cotton under SEM. These convolutions are present to a greater or lesser degree, depending on 1) the maturity of the cotton fibre at harvest; 2) the method by which a given sample of cotton was processed; and 3) the sample's state of degradation (Lukesova 2021; Suomela et al. 2023; Lukesova and Holst 2024). See **Figure 21** for an example of a modern cotton fibre viewed in longitudinal profile via SEM; convolutions are clearly visible. See **Figure 22** for an example of a heritage cotton fibre; again, the characteristic convolutions are visible — although, in this instance, the convolutions are more relaxed, for lack of a better term.

In **Figures 23** through **28** are presented 6 examples of the SEM images generated over the course of the present study. The images obtained reveal a consistent and distinctive surface morphology, apparent across the analysed textile fragments. Most significantly, the fibres exhibit ribbon-like forms with more or less regular longitudinal convolutions; these are especially visible in the better-preserved regions of the samples (see **Figure 26** and **28**). As stated above, the presence of these convolutions confirms that the samples under investigation are composed of cotton fibres as opposed to other plant-based fibres such as flax — which appear polygonal and smooth — or animal fibres such as wool — which exhibit characteristic scales (Gleba 2012; Markova 2019).

Despite the poor conservation status of the textile fragments, their distinctive, convoluted surface morphology is remarkably persistent. Nevertheless, the SEM images do reveal extensive evidence of deterioration. One consistent feature present in the majority of the samples is the presence of gaps or fissures running along the length of the fibres; these are particularly noticeable in **Figures 23** and **25**. Is it likely that these gaps are related to the post-depositional deterioration of the cotton fibre — by means of chemical degradation or mechanical stress — rather than the structure of the cotton itself (Cronyn 1990). Further evidence of deterioration is visible in **Figure 27**; here, the fibres appear frayed or indeed broken, indicating structural failure at the microfibrillar level. Finally, in the case of certain fragments, exogenous materials are clearly visible (see **Figures 23** through **25**); the presence of these materials may well have contributed to the physical and chemical breakdown of the sample surfaces.

Unsurprisingly, charging proved a major issue in obtaining suitable SEM imagery. The anomalous visual effects characteristic of the phenomenon are clearly visible in the **Figures 24** and **27**; here, the images contain bright, apparently over-exposed areas. Charging was largely unavoidable, but the effects thereof were mitigated by altering the accelerating voltage and the spot size.

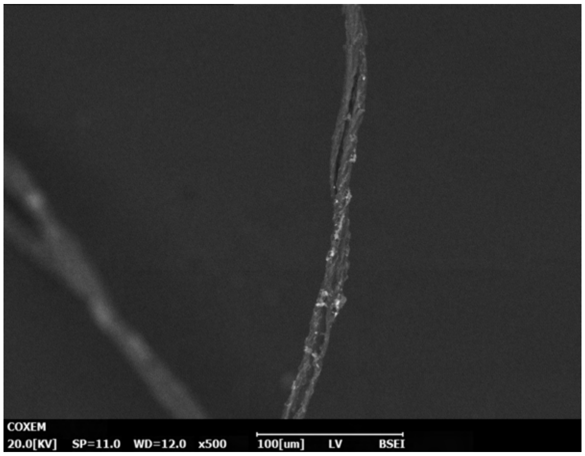

Figure 23: SEM micrograph of S211H310 Y2 at 500x magnification.

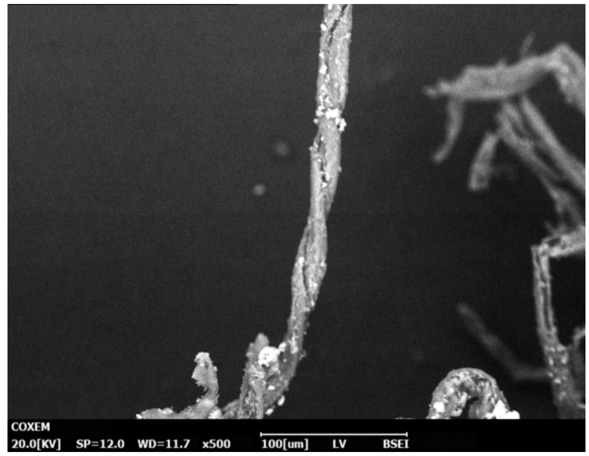

Figure 24: SEM micrograph of S192H275 Fragment 2 at 500x magnification.

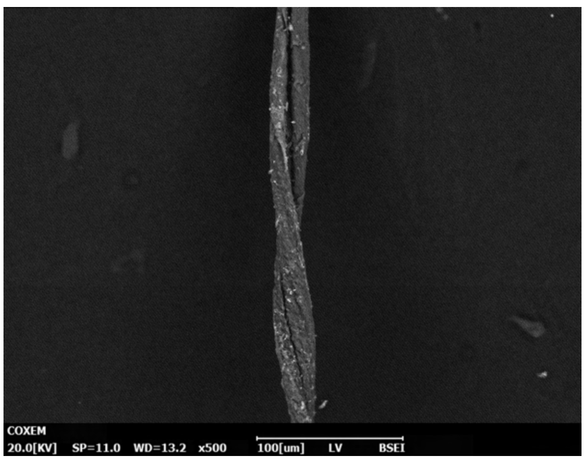

Figure 25: SEM micrograph of S196H282 Y1 at 500x magnification.

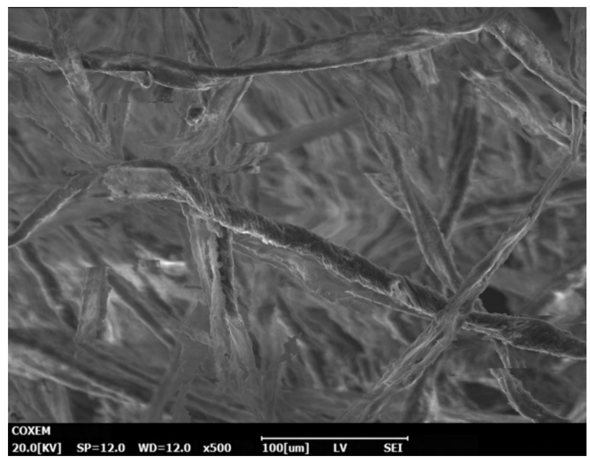

Figure 26: SEM micrograph of S196H282 Y2L Fragment 11 at 500x magnification.

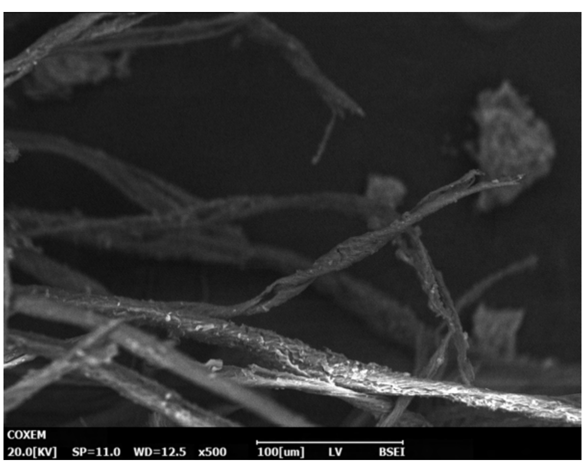

Figure 27: SEM micrograph of S211 H310 Y3 at 500x magnification.

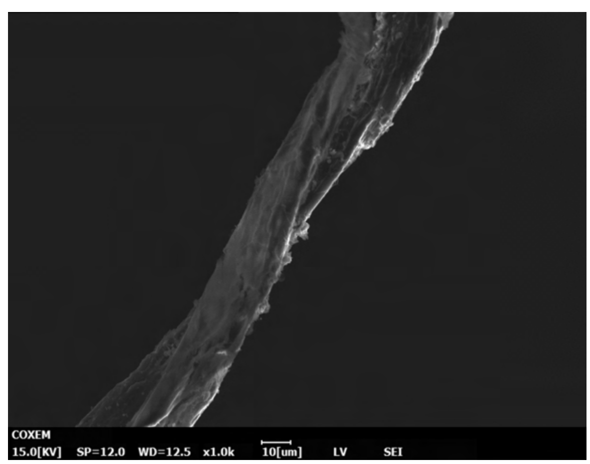

Figure 28: SEM micrograph of S196H282 Y2L Fragment 3 at 1000x magnification.

IV.3. Energy-dispersive X-ray spectroscopy (EDS)

EDS was applied to complement the morphological observations obtained through SEM analysis, as just detailed. While the latter technique permitted the structural identification of the cotton fibre — thereby providing detailed information on the material composition and conservation status of the textile fragments — EDS allowed for a more detailed understanding of the chemical composition of the surfaces of the fragments. EDS was carried out on 2 of the textile fragments previously examined under SEM: S192H275 Fragment 1 and S211H310 Y2. These samples were selected due to the presence of the greenish residue visible on their respective surfaces. The primary aim of carrying out EDS was to determine the elemental composition of this residue; more broadly, the aim was to identify any further evidence of degradation processes. To that end, using the AZtecTEM software, those locations on the surface of the samples exhibiting this residue were targeted for analysis using the EDS detector.

EDS yielded clear spectra indicating the presence of numerous metallic elements on both textile fragments, including: (Cu); potassium (K); and magnesium (Mg). Other non-metallic elements were also identified in various quantities, including: carbon (C); oxygen (O); nitrogen (N); calcium (Ca); silicon (Si); phosphorus (P); and chlorine (Cl). For a chart detailing the relative weights of those elements which were determined to be present, see **Figure 29.**

Sample ID	Cu	O	C	Cl	Mg	Si	Ca	P
S192H275 F1 Region 1	35.1–36.9	27.2–29.7	23.0–25.6	9.3-9.5	Not present	<0.5	<0.5	<0.5
S192H275 F1 Region 2	2.8–16.6	34.4–46.3	23.0–44.2	0.2-1.0	0.5-10.9	0.5-14.2	1.5–2.1	0.2–1.4
S192H275 F1 Region 3	3.3–9.6	27.2–40.2	40.9–56.4	0.4-1.1	≤0.5	0.2-4.2	1.4-4.7	0.3-3.1
S211H310 Y2	18.5–24.8	30.2–36.2	26.4–32.0	1.8-2.4	Not present	0.2-0.8	3.3-3.8	5.5–7.8

Figure 29: Range of relative weights (%) of Copper (Cu), Oxygen (O), Carbon (C), Chlorine (Cl), Magnesium (Mg), Silicon (Si), Calcium (Ca) and Phosphorus (P).

Elemental maps were generated in order to visualize the lateral distribution of these elements along the sample surfaces. The abundance of each element varied from one region of the given sample to the next, but copper was by and large the most abundant. This fact lends credence to the hypothesis advanced above — to wit, that the greenish residue visible on certain textile fragments is the result of copper-based corrosion products. In **Figures 30** through **33** are presented the results of EDS analysis, in the form of spectra and elemental maps.

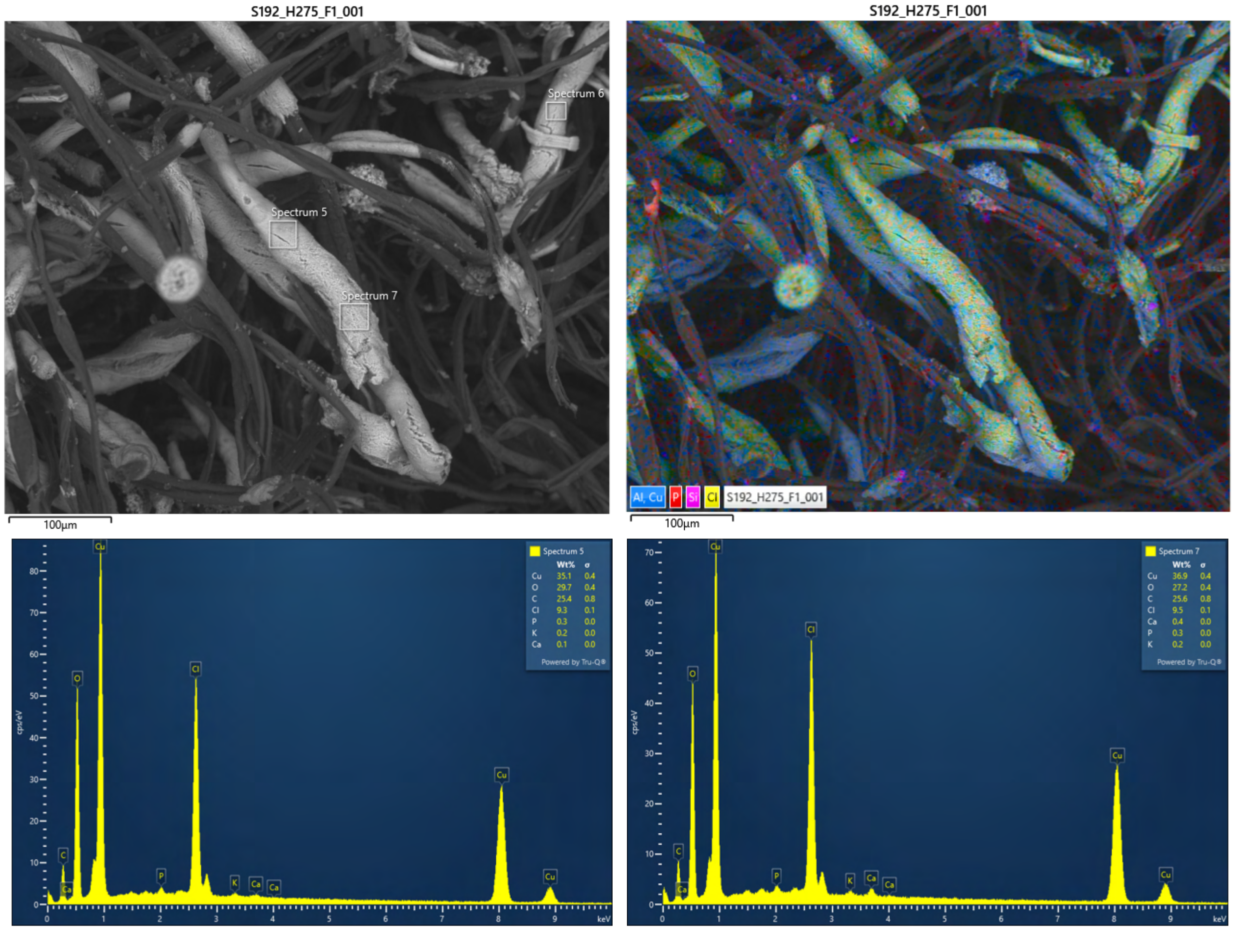

Figure 30: (Clockwise from top left) SEM-EDS image of S192H275 Fragment 1, region 1, with analysed regions indicated; elemental map of same; spectra obtained for these regions.

As indicated in **Figure 30**, copper was revealed to be the most abundant element in the first region of S192H275 Fragment 1, with a relative weight ranging from 35.1% to 36.9%. The second and third most abundant elements in this region of the fragment are oxygen (27.2-29.7%) and carbon (25.4-25.6%). The simultaneous presence of these three elements in significant quantities suggests the presence of copper carbonate ($CuCO_3$) compounds, a common class of corrosion products formed through the oxidative degradation of copper in post-depositional contexts (Oudbashi, Naseri, and Asadi Hasanvand 2024). One of the more surprising findings in this region of the fragment was the detection of a not insignificant percentage of chlorine, which stands at a relative weight of approximately 9.5% in both regions analyzed. The presence of this element may indicate the formation of copper chlorides as a degradation product — likely the result of deposition in a chlorine-rich environment (Scorr 1990).

The spectra obtained of the second region of S192H275 reveal a more heterogenous elemental composition. As indicated in **Figure 31**, EDS analysis again demonstrated an abundance of carbon (23.0-44.2%); oxygen (34.4%-46.3%); and copper (2.8%-16.6%). However, silicon, magnesium, nitrogen, and calcium are also present in various degrees; indeed, spectrum 10 revealed that, in at least one region of the sample, silicon and magnesium (14.2% and 10.9%, respectively) are significantly

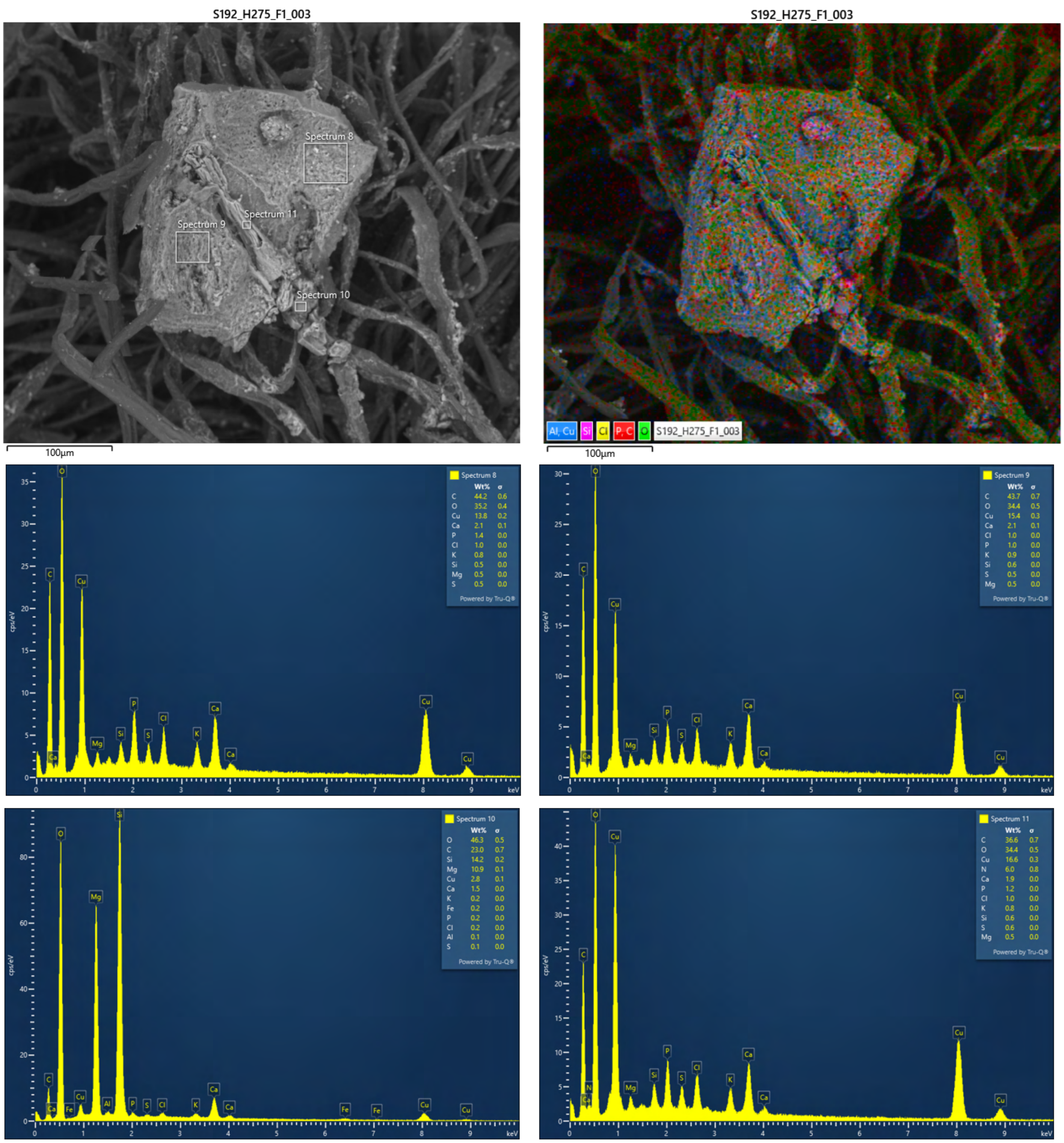

Figure 31: (Clockwise from top left) SEM-EDS image of S192H275 Fragment 1, region 2, with analysed regions indicated; elemental map of same; spectra obtained for these regions.

more abundant than was copper (2.8%). Furthermore, in all analysed regions, calcium is present in small quantities (1.5-2.1%), as is phosphorus (0.2-1.4%). The presence of these latter two elements is likely related to the breakdown of the bones of the buried individuals contained in the grave (Margariti et al. 2024). The presence of silicon is more difficult to explain, but is likely attributable to post-depositional soil contamination (Margariti et al. 2024).

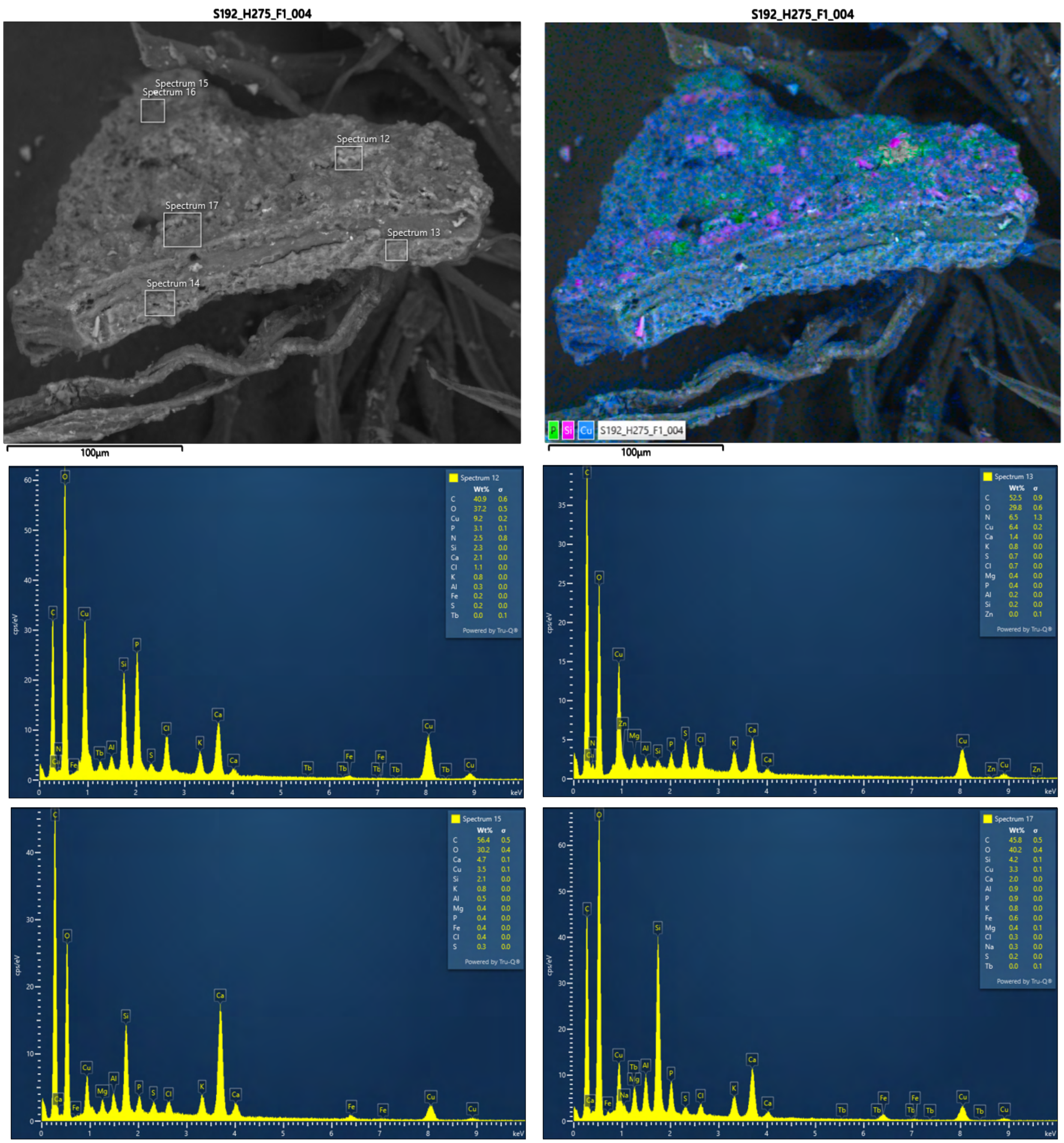

Figure 32: (Clockwise from top left) SEM-EDS image of S192H275 Fragment 1, region 3, with analysed regions indicated; elemental map of same; spectra obtained for these regions.

In **Figure 32** are reported the spectra and elemental maps obtained of the third and final region of S192H275 Fragment 1. The most abundant elements are carbon (40.9-56.4%) and oxygen (29.8-40.2%). Copper is less abundant than in the previous regions (3.3-9.2%), as are magnesium (0.0-0.4%) and silicon (0.7-4.2%). Interestingly, as is indicated in spectrum 15, calcium is the third most abundant

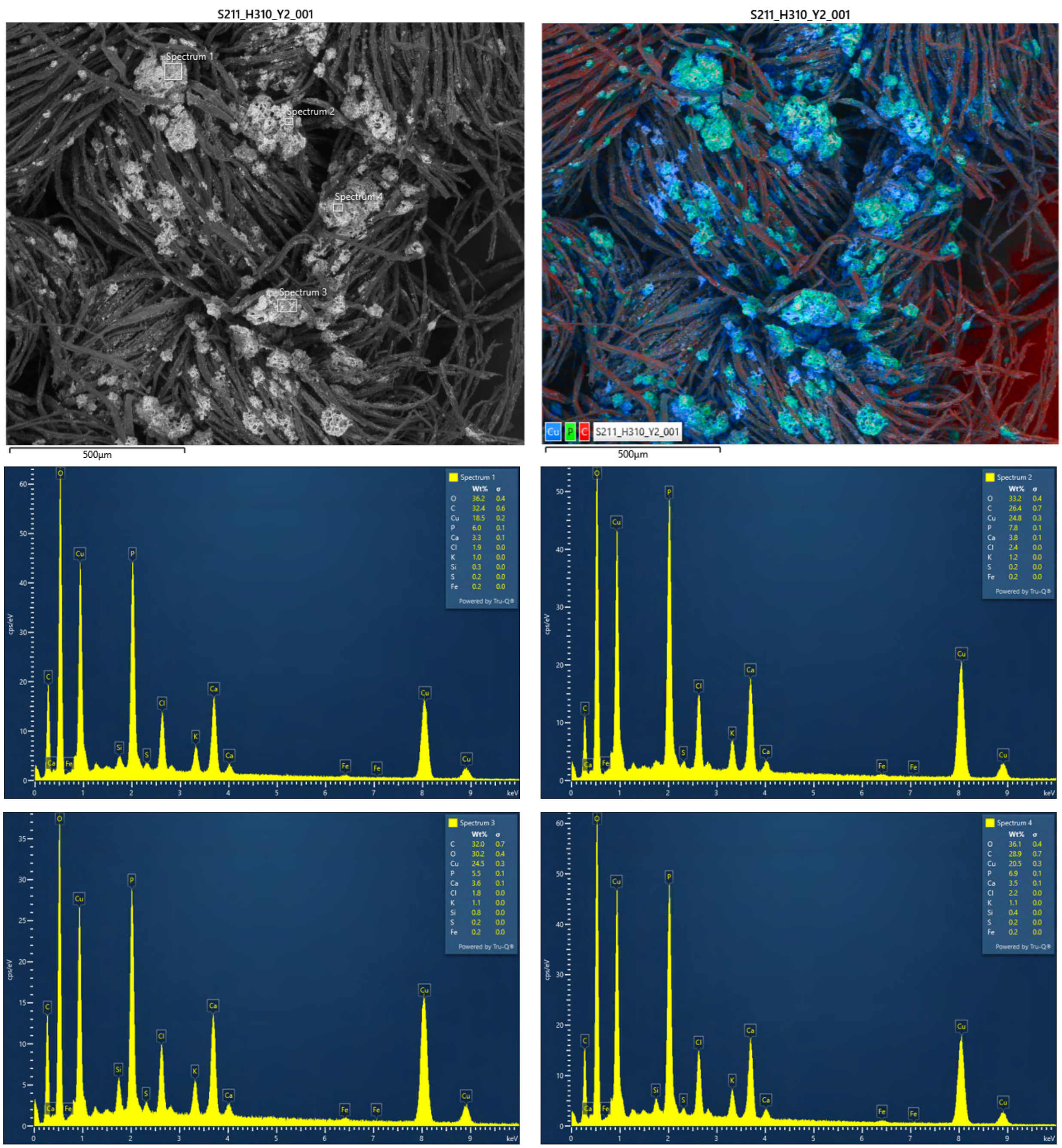

Figure 33: (Clockwise from top left) SEM-EDS image of S211H310 Y2 with analysed regions indicated; elemental map of same; spectra obtained for these regions.

element (4.7%) in at least one area of the sample surface. As in the previous region analysed, the presence of calcium is likely derived from the bones of the buried individuals.

Finally, in **Figure 33** are reported the data obtained for S211H310 Y2. The elemental composition of this fragment is more consistent than in the previous pieces; overwhelmingly, the most abundant elements present in all regions of this sample are oxygen (30.2-36.2%), carbon (25.4-30.2%), and copper (18.5-24.8%). Phosphorus (5.5-7.8%) occurs in all regions more or less consistently. The simultaneous presence of phosphorus and calcium may once again be derived from the bones of the buried individuals.

IV.4. Radiocarbon dating

The results of radiocarbon dating from KIK-IRPA are forthcoming.

V. Discussion

V.1. The physico-material perspective

In undertaking the suite of technical procedures detailed in the previous chapters, we have come closer to a comprehensive understanding of the structural parameters, material composition, and conservation status of the textile fragments under investigation. Structural textile analysis via autoptic observation and Dino-Lite digital microphotography permitted the detailed characterization of the fragments, that is, as balanced, plain-woven textiles of variable thread count, composed of z-twisted threads of variable diameter. Textile analysis also allowed for the identification of other diagnostic features — notably, sewn elements and possible degradation byproducts. The author recommends that the results obtained during structural textile analysis be complemented by a similar analysis of the other textile fragments discovered at Zeytinli Bahçe, which were not discussed here.

Moving forward, SEM generated high-resolution images of the textile fragments' surface morphology, thereby permitting the identification of the samples as cotton. However, the question remains as to which of the various species of the genus *Gossypium* was used to produce the textiles. Globally, there exist four domesticated cotton species of commercial significance: *G. arboreum*; *G. herbaceum*; *G. hirsutum*; and *G. barbadense* (Suomela et al. 2023). The anatomy and morphology of these distinct species differs the one from the other in fundamental ways; however, identifying and distinguishing between them remains difficult, even using SEM (Suomela et al. 2023; Lukesova and Holst 2024). With highly degraded samples such as those under examination here, the question of species identification is even more complicated. The author therefore recommends that further SEM imaging be undertaken, longitudinally and in cross section, both of which methods have proven instrumental for the identification of cotton species (Cao et al. 2009; Suomela et al. 2023; Lukesova and Holst 2024). The author confesses to having used only a small selection of the tools at the disposal of the archaeological microscopist; further measurement under SEM — for example, of thread twist and thread count — could very well yield important diagnostic information vis-à-vis fibre species identification (Cao et al. 2009).

Next, SEM was supplemented by the application of EDS; the data obtained by the latter technique support the claim that at least some of the textile fragments under investigation in the present work were deposited in contact with copper-based artefacts. This is consistent with field documentation noting that certain fragments were found in connection with metal ornaments — as well as the excavators' labelling some of the fragments in such a way as to suggest that these fragments, too, were found in connection with jewellery or ornamentation of some kind (Dell'Era 2012). The identification of copper carbonate, as well as numerous degradation products, also suggests that the depositional environment contributed to the physico-chemical transformation of the textiles and associated metallic components. The presence of silicon, calcium, and magnesium may be the result of post-depositional soil contamination, or indeed of post-excavation degradation processes; confirmation of such claims, however, would require geoarchaeological research into the soil conditions in the area surrounding Zeytinli Bahçe.

The author recommends that further EDS be conducted on the extant metal ornaments discovered in association with the textile fragments, and on any other metal artefacts excavated from the mediaeval funerary areas. Such an analysis could establish with greater certainty the connection between these artefacts and the corrosion products observed under EDS in the present study.

The present study will also benefit from the addition of radiocarbon dating results, which are currently pending. In providing an approximate date for the textile fragments making up the collection, these results will help to clarify the chronology of the mediaeval layers of Zeytinli Bahçe, and the site in general.

V.2. The historico-cultural perspective

The techniques just discussed provide vital information on the materiality of the textile fragments under investigation here; let us now broaden the scope of our analysis to encompass the larger historico-cultural context within which these textiles were originally produced.

The cultivation and consumption of cotton dates back thousands of years — perhaps as far back as 5000 B.C. (Barber 1991; Suomela et al. 2023). Archaeological evidence suggests that cotton domestication arose relatively simultaneously in both the Old and New Worlds; the fibre was in use in present-day Pakistan by the 6th millennium B.C., and present-day Mexico by the 4th millennium B.C. (Markova 2019). The use of cotton in western Asia and the Near East appears to have developed more recently, with archaeological cotton finds from Jordan dating to 4450-3000 B.C. at the earliest (Suomela et al. 2023).

Evidence of cotton cultivation in Anatolia dates to much later. While isolated cotton remains have been excavated from Hellenistic sites, these have been interpreted as potentially intrusive, and therefore do not constitute firm evidence of local cultivation (Marston and Castellano 2023). Indeed, the use of cotton in the region is not definitively attested to until the Middle Byzantine period, between the 9th and 13th centuries A.D.; archaeological findings indicate that this period likely represents the *terminus post quem* for the adoption of cotton in Anatolia (Marston and Castellano 2023). These findings would seem to align with Andrew Watson's thesis concerning the spread of cotton, to wit, that the crop was introduced into the Mediterranean as part of a wider 'agricultural revolution' engendered by the Islamic conquests of the late first millennium A.D. (Watson 1974, p.8; 1983; Kelley 2020).

Recent scholarship, however, has cast doubt on the diffusionist model advocated for by Watson. Basal et al. (2019) claim *Gossypium herbaceum L.* was most likely introduced to Anatolia from the Indian subcontinent circa the first century B.C. (Basal et al. 2019). Likewise, Kelley (2020) asserts that cotton was cultivated in certain areas of the Mediterranean — namely, North Africa, Egypt, and Central Asia — well before the Islamic conquests (Kelley 2020). Kelley's analysis of the relevant historical and archaeological data suggests that the crop was disseminated and adopted gradually — that is, at different rates in different regions — after its domestication in India. In light of these debates, the presence of cotton in mediaeval Anatolia likely reflects both diffusion through expanding networks of exchange and political power, and adaptation to local agricultural practices. Whether cotton was cultivated locally at Zeytinli Bahçe, however, remains an open question.

In their field reports for the 2001 and 2002 excavation campaigns at Zeytinli Bahçe, Frangipane et al. (2004; 2011) dedicate significant attention to the archaeological evidence of agricultural and industrial activity at the site. This discussion is limited, however, to the presence of faunal remains — with the aim of determining whether animal husbandry was practiced at the site — and evidence of metallurgy in the Bronze Age layers (Frangipane et al. 2004; Frangipane, Di Nocera, and Siracusano 2011). In addition to the archaeometric analyses already recommended, therefore, further archaeobotanical research is called for to ascertain whether cotton cultivation was practiced at the site, during the mediaeval period or earlier. Such research might shed light on the particular species of cotton making up the textiles under examination in this work; this might, in turn, permit the determination of whether these pieces are composed of local or imported varieties of the plant. Cotton textiles and raw cotton have been widely exchanged throughout Eurasia for thousands of years, and the discovery of cotton artefacts at Zeytinli Bahçe does not qualify as adequate evidence for cultivation of the plant (Mir-Makhamad et al. 2024). It should be noted, though, that bone and stone spindle whorls were discovered in the domestic areas located on the central cone and the slopes; it is unclear, however, whether these artefacts are contemporary with the textile fragments discovered in the cemetery

(Dell'Era 2012). None withstanding this question of dating, the presence of these tools suggests at minimum that fibre processing was practiced at the site.

The present study is hindered by the near-total lack of archaeological evidence as to the textile cultures which existed during the mediaeval period in this region; in general, so far as textiles are concerned, the archaeological record for the mediaeval Byzantine period is wanting (Linscheid 2012). This dearth of comparable finds represented the greatest obstacle to interpreting the textile fragments recovered at Zeytinli Bahçe. Comparisons with other mediaeval Byzantine textiles are not particularly insightful, insofar as such pieces are typically sourced from elite contexts, and composed of silk rather than cotton (Linscheid 2012). Indeed, silk may well be considered the representative fabric of the Byzantine empire; it was of such economic and cultural significance that, by the 6th century A.D., production was at least partially controlled by the Byzantine state (Fulghum 2001; Galliker 2014).

Despite the limitations of such an approach, and with little else to go on, it is instructive to begin by comparing the textile fragments discovered at Zeytinli Bahçe with artefacts retrieved from similar contexts in Anatolia. One potentially valuable source of information is Linscheid (2012); Linscheid details a number of archaeological textiles excavated from the Phrygian city of Amorium — including a selection of fragments retrieved from Christian tombs dated to the second half of the 10th century A.D. These fragments are highly degraded and have not been fully analysed, but their archaeological context is remarkably clear. Of note are the pieces discovered in Tomb no. 6, Burial no. 1; these consist of a plain-woven, embroidered silk burial shroud, a cord used to secure the shroud to the body of the deceased, and remnants of outer garments, including shoes (Linscheid 2012). These pieces are composed of silk, rather than cotton; the tombs have therefore been interpreted as belonging to the Christian aristocracy of Amorium (Linscheid 2012). Nonetheless, these findings offer a useful point of comparison with those retrieved from Zeytinli Bahçe — both in terms of their chronological proximity, and the similarity of the contexts in which they were found. Indeed, despite their having been deposited in a high-status burial, the textiles from Amorium testify to the use of cotton in both quotidian and more ritualistic contexts, thereby reinforcing the possibility that the textiles discovered at Zeytinli Bahçe reflect broader, interregional patterns of exchange and religious practice.

Another relevant comparative source of information is Shamir (2019), which text serves as a précis of thousands of textiles and textile fragments found in modern-day Israel and the Palestinian territories, dating from the pre-pottery Neolithic unto the mediaeval period. Of particular interest are a collection of textile fragments discovered in a Christian cemetery at Qasr el-Yahud, on the western banks of the

Jordan. These fragments serve as rare evidence, archaeological or otherwise, of Christian burial practices during the 8th and 9th centuries A.D. (Shamir 2019). The pieces were found in direct contact with the individuals buried in the cemetery; they include tunics, head coverings, bandages, and shrouds (Shamir 2019). Archaeological and anthropological analysis of the textile fragments uncovered at Qasr el-Yahud has led researchers to conclude that they are of foreign manufacture, and likely imported into Palestine (Shamir 2019).

Structurally, the textile fragments from Qasr el-Yahud differ from those found at Zeytinli Bahçe in several respects. Whereas all of the samples analysed in the present study were identified be cotton-based, only a small number of the pieces recovered from Qasr el-Yahud — 85 out of a total of 250 fragments — were so identified (Shamir 2019). Moreover, the fragments from Qasr el-Yahud exhibit substantial variation in thread twist direction; most are s-spun in the warp, and s-spun in the weft. This is, of course, in contrast with the pieces found at Zeytinli Bahçe, all of which were z-spun in both systems. This latter distinction could well prove significant for the identification of the cotton's provenance; Kelley (2020) asserts that z-spun cotton threads are interpreted as being Indian in origin, s-spun cotton threads as being African in origin. As stated above, however, more detailed analysis is required to definitively prove or disprove this apparent pattern.

As with the fragments excavated at both Amorium and Qasr el-Yahud, those excavated at Zeytinli Bahçe were found deposited in a funerary context. The use of textiles in such contexts is an ancient, long-lived practice observed in diverse cultures and locales, from Ancient Egypt to pre-Columbian North America (Barber 1991). Taken together, the case studies presented here provide insight into the kinds of textiles circulating in the eastern Mediterranean during the mediaeval period, as well as the roles such textiles played in funerary rites, and in everyday life. They attest further to the broader networks — economic, cultural, and religious — which shaped the production, exchange, and use of textiles in this period. As we have seen, it is exquisitely rare to come upon these sorts of textiles in the archaeological record; where they do occur, it is important that they be subject to the appropriate archaeometric and technical analyses. Working from these fragmented bits of information, our understanding of textiles and material culture — in mediaeval Anatolia and beyond — might come into clearer focus.

VI. Conclusion

Over the course of the present study, a collection of 26 textile fragments from Zeytinli Bahçe was observed, documented, and analysed by a suite of techniques. As detailed in the preceding chapters, these techniques were successful in describing the structural parameters of the textile fragments; identifying the type of fibre used to produce them; characterizing the elemental composition of the surfaces of the pieces sampled; and determining what degradation products are present thereupon. Apart from the recommendations advanced in the previous chapters, the author suggests that the present work — and the field of textile archaeology as a whole — would benefit from the expansion and consolidation of extant textile databases. Such databases, such as the Old World Crops Archaeobotanical Database, do exist, but they remain either unfinished or inaccessible to the general researcher (Fuller et al. 2024). The availability of historic data on the distribution of archaeological textile finds is integral to studies such as this, insofar as they permit comparisons to be drawn between artefacts deriving from different regions and time periods. Indeed, as already stated, the general lack of comparable artefacts proved perhaps the greatest obstacle to the author in preparing the present work.

With that in mind, the author would conclude by underscoring the particular difficulty faced by researchers working with archaeological textiles. Absent primary sources, and with scant physical evidence to go by, the cautious textile archaeologist is confronted with the unnerving possibility that it is indeed impossible to contextualize the objects which they have chosen to study.

The multidisciplinary investigation of archaeological textiles, of course, represents a new front in the larger field of textile archaeology. Indeed, it would appear as if the integration of technical analysis with ostensibly conventional archaeological techniques — stratigraphy, stylistic analysis, and typology, for example — permits a more cohesive reconstruction of the history of archaeological objects, as well as a more comprehensive understanding of the materials used to create them (cf. Artioli 2010). By applying so integrative a method, the textile archaeologist would seem to occupy a more favourable position than it may appear.

The question remains, though, whether these diverse methods can be used to answer the sorts of questions which archaeology aims to answer. In the context of the present study, the most pressing of these questions is: *what were these textile fragments?* Unfortunately, no matter the magnification of the microscope employed — no matter how expertly calibrated this or that instrument may be — we have come only a bit closer to answering this question than when we began. We can conclude by saying the only the following. The textile fragments discovered at Zeytinli Bahçe are composed of plain-woven cotton, as demonstrated by Dino-Lite digital microphotography and SEM. These fragments exhibit evidence of deterioration — either by corrosion processes, or post-depositional contamination — as demonstrated by EDS. Insofar as they were discovered in a cemetery, it is likely that the fragments are grave goods; insofar as the corrosion products present on the fragments match those typically found in connection with metal artefacts, it is likely that they were also deposited in connection with such artefacts. Beyond this lies the realm of speculation.

Appendix: Sample catalogue

The following catalogue contains is organized after the convention set by the original excavators, to wit: the individual pieces are categorized by coordinates within the excavation grid, followed by burial number (indicated by 'S' [*sepoltura*]), and buried individual (indicated by 'H' ['*homo*']). They are further subdivided according to the descriptions enclosed with the fragments by the original excavators (see **Chapter II**). The 26 textile fragments are divided into five assemblages: S185H268 (consisting of 2 fragments); S192H275 (2 fragments); S196H282 (16 fragments, subdivided into 3 groups [Y1; Y2; and Y2L]); S208H305 (2 fragments, subdivided into 3 groups [Y1; and Y2]) and S196H282 (4 fragments, subdivided into 3 groups [Y1; Y2; and Y3]).

The catalogue contains entries for each of the 26 fragments, save for those associated with S208H305, which were determined to consist entirely of exogenous materials. For the remaining 24 fragments in the collection, the following data are provided: length in centimetres; width in centimetres; weave type; thread twist direction; average thread diameter of systems 1 and 2, in millimetres; and thread counts of system 1 and 2. As noted above, these measurements should be considered provisional.

Unless otherwise marked, the photographs presented in the catalogue were taken by Dr. Emanuela Faresin on the premises of University of Padova's *Laboratori di Archeologia*. The Dino-Lite microphotographs were acquired by the author over the course of structural textile analysis.

E7(15) S185H268
Fragment 1

Tessuto sotto anello Y2

Length (cm)	Width (cm)	Weave	Twist
1	0.8	Plain	z

Sys. 1 thread count	Sys. 2 thread count	Sys. 1 avg. thread diameter (mm)	Sys. 2 avg. thread diameter (mm)
12(?)	14	0.33	0.41

Top: photograph by E. Faresin.
Bottom: Dino-Lite image at 50x magnification.

E7(15) S185H268
Fragment 1

Tessuto sotto anello Y2

Length (cm)	Width (cm)	Weave	Twist
1.7*	1.2*	n/d	z

Sys. 1 thread count	Sys. 2 thread count	Sys. 1 avg. thread diameter (mm)	Sys. 2 avg. thread diameter (mm)
n/d	n/d	n/d	n/d

*The fragment consists of 2 pieces; measurements for the larger piece are provided.

Top: photograph by E. Faresin.
Bottom: Dino-Lite image at 50x magnification.

E7(15)/E8(3)
S192H275 Fragment 1

Tessuto sotto anello Y1

Length (cm)	Width (cm)	Weave	Twist
n/d	n/d	Plain	z

Sys. 1 thread count	Sys. 2 thread count	Sys. 1 avg. thread diameter (mm)	Sys. 2 avg. thread diameter (mm)
14	22	0.38	0.27

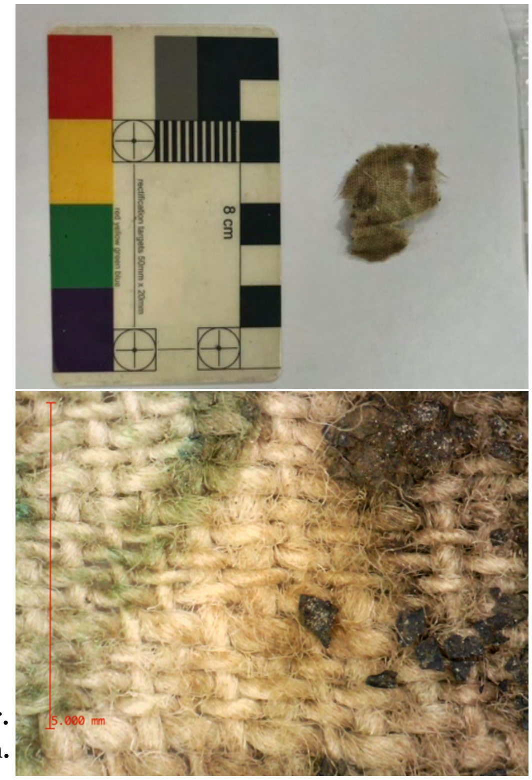

Top: photograph by the author.
Bottom: Dino-Lite image at 50x magnification.

E7(15)/E8(3)
S192H275 Fragment 2

Tessuto sotto anello Y1

Length (cm)	Width (cm)	Weave	Twist
3.2	2.3	Plain	z

Sys. 1 thread count	Sys. 2 thread count	Sys. 1 avg. thread diameter (mm)	Sys. 2 avg. thread diameter (mm)
18(?)	20(?)	0.37	0.39

Top: photograph by E. Faresin.
Bottom: Dino-Lite image at 50x magnification.

E8(3/4)
S196H282 Y1

Tessuto sotto Y1 (anello) con costole

Length (cm)	Width (cm)	Weave	Twist
2.1	0.7	Plain	z

Sys. 1 thread count	Sys. 2 thread count	Sys. 1 avg. thread diameter (mm)	Sys. 2 avg. thread diameter (mm)
14	16	0.56	0.67

Top: photograph by E. Faresin.
Bottom: Dino-Lite image at 50x magnification.

E8(3/4)
S196H282 Y2 Fragment 1

Sotto bracciale destro Y2

Length (cm)	Width (cm)	Weave	Twist
7	5.4	Plain	z

Sys. 1 thread count	Sys. 2 thread count	Sys. 1 avg. thread diameter (mm)	Sys. 2 avg. thread diameter (mm)
12	12	0.56	0.67

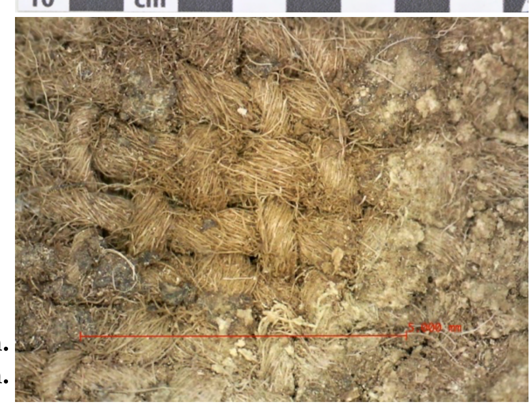

Top: photograph by E. Faresin.
Bottom: Dino-Lite image at 50x magnification.

E8(3/4)
S196H282 Y2 Fragment 2

Sotto bracciale destro Y2

Length (cm)	Width (cm)	Weave	Twist
4.1	1	Plain	z

Sys. 1 thread count	Sys. 2 thread count	Sys. 1 avg. thread diameter (mm)	Sys. 2 avg. thread diameter (mm)
10(?)	n/d	0.61	0.79

Top: photograph by E. Faresin.
Bottom: Dino-Lite image at 50x magnification.

E8(3/4)
S196H282 Y2 Fragment 3

Sotto bracciale destro Y2

Length (cm)	Width (cm)	Weave	Twist
1.4	0.8	Plain	z

Sys. 1 thread count	Sys. 2 thread count	Sys. 1 avg. thread diameter (mm)	Sys. 2 avg. thread diameter (mm)
12	10	0.52	0.74

Top: photograph by E. Faresin.
Bottom: Dino-Lite image at 50x magnification.

E8(3/4)
S196H282 Y2 Fragment 4

Sotto bracciale destro Y2

Length (cm)	Width (cm)	Weave	Twist
0.6	2	Plain	z

Sys. 1 thread count	Sys. 2 thread count	Sys. 1 avg. thread diameter (mm)	Sys. 2 avg. thread diameter (mm)
16	16-18(?)	0.45	0.42

Top: photograph by E. Faresin.
Bottom: Dino-Lite image at 50x magnification.

E8(34)
S196H282 Y2L Fragment 1

Sotto Y2L

Length (cm)	Width (cm)	Weave	Twist
2.9	2	Plain	z

Sys. 1 thread count	Sys. 2 thread count	Sys. 1 thread diameter (mm)	Sys. 2 thread diameter (mm)
15	14	0.48	0.52

Top: photograph by E. Faresin.
Bottom: Dino-Lite image at 50x magnification.

E8(34)
S196H282 Y2L Fragment 2

Sotto Y2L

Length (cm)	Width (cm)	Weave	Twist
2.7	1.8	Plain	z

Sys. 1 thread count	Sys. 2 thread count	Sys. 1 avg. thread diameter (mm)	Sys. 2 avg. thread diameter (mm)
16	16	0.51	0.53

Top: photograph by E. Faresin.
Bottom: Dino-Lite image at 50x magnification.

E8(34)
S196H282 Y2L Fragment 3

Sotto Y2L

Length (cm)	Width (cm)	Weave	Twist
2	1.5	Plain	z

Sys. 1 thread count	Sys. 2 thread count	Sys. 1 avg. thread diameter (mm)	Sys. 2 avg. thread diameter (mm)
14(?)	16(?)	0.45	0.36

Top: photograph by E. Faresin.
Bottom: Dino-Lite image at 50x magnification.

E8(34)
S196H282 Y2L Fragment 4

Sotto Y2L

Length (cm)	Width (cm)	Weave	Twist
1.8	2	Plain	z

Sys. 1 thread count	Sys. 2 thread count	Sys. 1 avg. thread diameter (mm)	Sys. 2 avg. thread diameter (mm)
12	12	0.49	0.62

Top: photograph by E. Faresin.
Bottom: Dino-Lite image at 50x magnification.

E8(34)
S196H282 Y2L Fragment 5

Sotto Y2L

Length (cm)	Width (cm)	Weave	Twist
1.6*	0.6*	Plain(?)	z

Sys. 1 thread count	Sys. 2 thread count	Sys. 1 avg. thread diameter (mm)	Sys. 2 avg. thread diameter (mm)
8(?)	n/d	n/d	n/d

*The fragment consists of 2 pieces; measurements for the larger piece are provided.

Top: photograph by E. Faresin.
Bottom: Dino-Lite image at 50x magnification.

E8(34)
S196H282 Y2L Fragment 6

Sotto Y2L

Length (cm)	Width (cm)	Weave	Twist
1.9	0.6	Plain(?)	z/i(?)

Sys. 1 thread count	Sys. 2 thread count	Sys. 1 avg. thread diameter (mm)	Sys. 2 avg. thread diameter (mm)
10(?)	10(?)	n/d	n/d

Top: photograph by E. Faresin.
Bottom: Dino-Lite image at 50x magnification.

E8(34)
S196H282 Y2L Fragment 7

Sotto Y2L

Length (cm)	Width (cm)	Weave	Twist
0.6*	0.7*	Plain(?)	z

Sys. 1 thread count	Sys. 2 thread count	Sys. 1 avg. thread diameter (mm)	Sys. 2 avg. thread diameter (mm)
n/d	n/d	n/d	n/d

*The fragment consists of 3 pieces; measurements for the largest piece are provided.

Top: photograph by E. Faresin.
Bottom: Dino-Lite image at 50x magnification.

E8(34)
S196H282 Y2L Fragment 8

Sotto Y2L

Length (cm)	Width (cm)	Weave	Twist
1.2	<0.5	Plain	x

Sys. 1 thread count	Sys. 2 thread count	Sys. 1 avg. thread diameter (mm)	Sys. 2 avg. thread diameter (mm)
12(?)	12(?)	0.61	0.54

Top: photograph by E. Faresin.
Bottom: Dino-Lite image at 50x magnification.

E8(34)
S196H282 Y2L Fragment 9

Sotto Y2L

Length (cm)	Width (cm)	Weave	Twist
1	<0.5	n/d	z(?)

Sys. 1 thread count	Sys. 2 thread count	Sys. 1 avg. thread diameter (mm)	Sys. 2 avg. thread diameter (mm)
10(?)	12(?)	0.51	0.66

Top: photograph by the author.
Bottom: Dino-Lite image at 50x magnification.

E8(34)
S196H282 Y2L Fragment 10

Sotto Y2L

Length (cm)	Width (cm)	Weave	Twist
0.5	<0.5	n/d	n/d

Sys. 1 thread count	Sys. 2 thread count	Sys. 1 avg. thread diameter (mm)	Sys. 2 avg. thread diameter (mm)
n/d	n/d	n/d	n/d

Top: photograph by the author.
Bottom: Dino-Lite image at 50x magnification.

E8(34)
S196H282 Y2L Fragment 11

Sotto Y2L

Length (cm)	Width (cm)	Weave	Twist
0.5	<0.5	n/d	z(?)

Sys. 1 thread count	Sys. 2 thread count	Sys. 1 avg. thread diameter (mm)	Sys. 2 avg. thread diameter (mm)
n/d	n/d	n/d	n/d

Top: photograph by E. Faresin.
Bottom: Dino-Lite image at 50x magnification.

E7(15)/E8(3)
S211H310 Y1 Fragment 1

Sotto Y1

Length (cm)	Width (cm)	Weave	Twist
<0.5	<0.5	n/d	n/d

Sys. 1 thread count	Sys. 2 thread count	Sys. 1 avg. thread diameter (mm)	Sys. 2 avg. thread diameter (mm)
n/d	n/d	n/d	n/d

Images unavailable.

E7(15)/E8(3)
S211H310 Y1 Fragment 2

Sotto Y1

Length (cm)	Width (cm)	Weave	Twist
n/d	n/d	n/d	n/d

Sys. 1 thread count	Sys. 2 thread count	Sys. 1 avg. thread diameter (mm)	Sys. 2 avg. thread diameter (mm)
n/d	n/d	n/d	n/d

Images unavailable.

E7(15)/E8(3)
S211H310 Y2

Sotto Y2

Length (cm)	Width (cm)	Weave	Twist
0.9	1	Plain	z

Sys. 1 thread count	Sys. 2 thread count	Sys. 1 avg. thread diameter (mm)	Sys. 2 avg. thread diameter (mm)
10	14	0.46	0.57

Top: photograph by the author.
Bottom: Dino-Lite image at 50x magnification.

E7(15)/E8(3)
S211H310 Y3

Vicino Y3

Length (cm)	Width (cm)	Weave	Twist
1	<0.5	Plain	z

Sys. 1 thread count	Sys. 2 thread count	Sys. 1 avg. thread diameter (mm)	Sys. 2 avg. thread diameter (mm)
14	16(?)	0.56	0.44

Top: photograph by the author.
Bottom: Dino-Lite image at 50x magnification.

Bibliography

Alvaro, Corrado, Francesca Balossi, and Joanita Vroom. 2004. "Zeytinli Bahçe. A Medieval Fortified Settlement." *Anatolia Antiqua* 12 (1): 191–213. https://doi.org/10.3406/anata.2004.1025.

Artioli, Gilberto. 2010. *Scientific Methods and Cultural Heritage : An Introduction to the Application of Materials Science to Archaeometry and Conservation Science*. Oxford: Oxford University Press.

Barber, E.J.W. 1991. *Prehistoric Textiles: The Development of Cloth in the Neolithic and Bronze Ages*. Princeton: Princeton University Press.

Basal, Huseyin, Emine Karademir, Hatice Kubra Goren, Volkan Sezener, Mehmet Nedim Dogan, Ibrahim Gencsoylu, and Oktay Erdogan. 2019. "Cotton Production in Turkey and Europe." In *Cotton Production*, edited by Khawar Jabran and Bhagirath Singh Chauhan, 1st ed., 297–321. Wiley. https://doi.org/10.1002/9781119385523.ch14.

Bender Jørgensen, L. 2004. "A Matter of Material: Changes in Textiles from Roman Sites in Egypt's Eastern Desert." *Antiquité Tardive* 12:87–99.

Bronk Ramsey, C. 2008. "RADIOCARBON DATING: REVOLUTIONS IN UNDERSTANDING*." *Archaeometry* 50 (2): 249–75. https://doi.org/10.1111/j.1475-4754.2008.00394.x.

Cao, Sukang Zhu, Ning Pan, Zhu Yuping, and Hengxian Tu. 2009. "Characterization of Archaeological Cotton (G. Herbaceum) Fibers from Yingpan." *Technical Briefs in Historical Archaeology* 4:18–28.

Coletti, Francesca, Christina Margariti, Vanessa Forte, and Stella Spantidaki, eds. 2024. *Multidisciplinary Approaches for the Investigation of Textiles and Fibres in the Archaeological Field*. Interdisciplinary Contributions to Archaeology. Cham: Springer Nature Switzerland. https://doi.org/10.1007/978-3-031-73812-8.

Cronyn, J.M. 1990. *Elements of Archaeological Conservation*. New York: Routledge.

Decker, Michael. 2007. "Frontier Settlement and Economy in the Byzantine East." *Dumbarton Oaks Papers* 61:217–67.

Dell'Era, Francesca. 2012. "Small Finds from Zeytinli Baçe - Birecik (Urfa)." In *Byzantine Small Finds in Archaeological Contexts*, 393–406. BYZAS 15. Istanbul: Ege Yayınları.

Dickey, Alistair. 2022. "EDS Analysis of Neolithic to Early Dynastic Egyptian Woven Cloth in the Bolton Museum Collection." In *Exploring Ancient Textiles: Pushing the Boundaries of Established Methodologies*, 93–109. Oxford and Philadelphia: Oxbow Books.

Emery, Irene. 1995. *The Primary Structures of Fabrics: An Illustrated Classification*. New York: Watson-Guptill Publications.

Frangipane, Marcella, Francesca Balossi R., Gian Maria Di Nocera, Alberto Palmieri, and Giovanni Siracusano. 2004. "The 2001 Excavation Campaign at Zeytinlibahçe Höyük: Preliminary Results." In *Salvage Project of the Archaeological Heritage of the Ilsu and Carchemish Dam Reservoirs Activities in 2001*, 1–56. Orta Dogu Teknik Universitesi.

Frangipane, Marcella, Gian Maria Di Nocera, and Giovanni Siracusano. 2011. "THE INVESTIGATIONS AT ZEYTINLIBAHCE HÖYÜK (URFA) THE 2002 CAMPAIGN." In *Salvage Project of the Archaeological Heritage of the Ilsu and Carchemish Dam Reservoirs Activities in 2002*, 1–34. Orta Dogu Teknik Universitesi.

Fulghum, Mary Margaret. 2001. "Under Wraps: Byzantine Textiles as Major and Minor Arts." *Studies in the Decorative Arts* 9 (1): 13–33. https://doi.org/10.1086/studdecoarts.9.1.40662797.

Fuller, Dorian Q, Louis Champion, Cristina Cobo Castillo, and Anna Den Hollander. 2024. "Cotton and Post-Neolithic Investment Agriculture in Tropical Asia and Africa, with Two Routes to West Africa." *Journal of Archaeological Science: Reports* 57 (September):104649. https://doi.org/10.1016/j.jasrep.2024.104649.

Galliker, Julia L. 2014. "Middle Byzantine Silk in Context: Integrating the Textual and Material Evidence." Bermingham: University of Birmingham.

Gigilashvili, Davit, Hana Lukesova, and Jon Yngve Hardeberg. 2024. "Criteria for Matching Fragmented Archaeological Textiles: A Survey." *Archaeological Textiles Review*, no. 66.

Gillis, Carole, and Marie-Louise Nosch. 2007. *First Aid for the Excavation of Archeological Textiles*. Oxbow Books. https://www.academia.edu/19433987/First_Aid_for_the_Excavation_of_Archeological_Textiles_2007.

Gleba, Margarita. 2012. “From Textiles to Sheep: Investigating Wool Fibre Development in Pre-Roman Italy Using Scanning Electron Microscopy (SEM).” *Journal of Archaeological Science* 39 (12): 3643–61. https://doi.org/10.1016/j.jas.2012.06.021.

———. 2017a. “TEXTILES IN PRE-ROMAN ITALY: FROM A QUALITATIVE TO A QUANTITATIVE APPROACH.” *Origini* XL:9–28. https://doi.org/10.17863/CAM.20482.

———. 2017b. “Tracing Textile Cultures of Italy and Greece in the Early First Millennium BC.” *Antiquity* 91 (359): 1205–22. https://doi.org/10.15184/aqy.2017.144.

———. 2020. “Unraveling the Fabric of the Past.” In *A Companion to Textile Culture*, 11–25. Wiley-Blackwell.

Gleba, Margarita, and Ulla Mannering. 2012. “Introduction: Textile Preservation, Analysis and Technology.” In *Textiles and Textile Production in Europe from Prehistory to AD 400*, 1–24. Oxford and Oakville: Oxbow Books. http://choicereviews.org/review/10.5860/CHOICE.50-1554.

HAMM. 2014. *Handbook for Analytical Methods for Materials*. Plymouth, MN: Materials Evaluation and Engineering Inc. (MEE). http://www.cientificosaficionados.com/microscopio/MICROSCOPIO%20ELECTRONICO_archivos/hamm72d.pdf.

Hammarlund, Lena. 2005. “Handicraft Knowledge Applied to Archaeological Textiles.” *The Nordic Textile Journal*, 87–119.

Kelley, Anna. 2020. “By Land or by Sea: Tracing the Adoption of Cotton in the Economies of the Mediterranean.” In *Transmitting and Circulating the Late Antique and Byzantine Worlds*, edited by Mirela Ivanova and Hugh Jeffrey, 274–97. Leiden & Boston: Brill. https://doi.org/10.1163/9789004409460.

Kutschera, Walter. 2016. “Accelerator Mass Spectrometry: State of the Art and Perspectives.” *Advances in Physics: X* 1 (4): 570–95. https://doi.org/10.1080/23746149.2016.1224603.

Linscheid, Petra. 2012. “Middle Byzantine Textile Finds from Amorium.” In *Byzantine Small Finds in Archaeological Contexts*, 343–50. BYZAS 15. İstanbul: Ege Yayınları.

Lukesova, Hana. 2021. “Fibres in Heritage Objects Identification and Characterisation by Imaging Techniques.” PhD Thesis, Bergen: University of Bergen.

Lukesova, Hana, and Bodil Holst. 2024. “Identifying Plant Fibres in Cultural Heritage with Optical and Electron Microscopy: How to Present Results and Avoid Pitfalls.” *Heritage Science* 12 (1): 12. https://doi.org/10.1186/s40494-023-01122-z.

Margariti, Christina, Gabriela Sava, Tiberiu Sava, Mathieu Boudin, and Marie-Louise Nosch. 2023. “Radiocarbon Dating of Archaeological Textiles at Different States of Preservation.” *Heritage Science* 11 (1): 44. https://doi.org/10.1186/s40494-023-00867-x.

Margariti, Christina, Gabriela Sava, Ina Vanden Berghe, and Daphne Filiou. 2024. “Exploring the Provenance of a Byzantine Excavated Assemblage of Textile and Leather Finds by the Application of Instrumental Analysis.” *Heritage Science* 12 (1): 132. https://doi.org/10.1186/s40494-024-01201-9.

Markova, Ivana. 2019. *Textile Fiber Microscopy: A Practical Approach*. 1st ed. Wiley. https://doi.org/10.1002/9781119320029.

Marston, John M., and Lorenzo Castellano. 2023. “Crop Introductions and Agricultural Change in Anatolia during the Long First Millennium Ce.” *Vegetation History and Archaeobotany*, May. https://doi.org/10.1007/s00334-023-00919-z.

Mir-Makhamad, Basira, Rasmus Bjørn, Kseniia Boxleitner, and Robert N. Spengler. 2024. “The Cotton Road: The History of an Exchange Commodity in Central Asia.” *Inner Asia* 26 (2): 193–230. https://doi.org/10.1163/22105018-02602002.

Netherton, Robin, and Gale R. Owen-Crocker, eds. 2008. *Medieval Clothing and Textiles*. 1st ed. The Boydell Press. https://doi.org/10.5040/9781800108356.

Nissen, Hans Jörg, Elizabeth Lutzeier, and Kenneth J. Northcott. 1988. *The Early History of the Ancient Near East, 9000-2000 B.C.* Chicago: University of Chicago Press.

Pollard, Nigel. 2000. *Soldiers, Cities, and Civilians in Roman Syria*. Ann Arbor: University of Michigan Press.

Ponting, Matthew. 2004. “The Scanning Electron Microscope and the Archaeologist.” *Physics Education* 39 (2): 166–70. https://doi.org/10.1088/0031-9120/39/2/004.

Rast-Eicher, Annette. 2016. *Fibres: Microscopy of Archaeological Textiles and Furs*. Budapest: Archaeolingua Alapítvány.

Rezić, Iva, Lidija Ćurković, and Magdalena Ujević. 2010. “Simple Methods for Characterization of Metals in Historical Textile Threads.” *Talanta* 82 (1): 237–44. https://doi.org/10.1016/j.talanta.2010.04.028.

Scorr, DAVID A. 1990. “Bronze Disease: A Review of Some Chemical Problems and the Role of Relative Humidity.”

Shaffner, T J, and R D Van Veld. 1971. “‘Charging’ Effects in the Scanning Electron Microscope.” *Journal of Physics E: Scientific Instruments* 4 (9): 633–37. https://doi.org/10.1088/0022-3735/4/9/002.

Shamir, Orit. 2019. “Cotton Textiles from the Byzantine Period to the Medieval Period in Ancient Palestine.” *Revue d’ethnoécologie*, no. 15 (June). https://doi.org/10.4000/ethnoecologie.4176.

Suomela, Jenni A., Mira Viljanen, Kirsi Svedström, Krista Wright, and Sanna Lipkin. 2023. “Research Methods for Heritage Cotton Fibres: Case Studies from Archaeological and Historical Finds in a Finnish Context.” *Heritage Science* 11 (1): 175. https://doi.org/10.1186/s40494-023-01022-2.

Synal, Hans-Arno, Martin Stocker, and Martin Suter. 2007. “MICADAS: A New Compact Radiocarbon AMS System.” *Nuclear Instruments and Methods in Physics Research Section B: Beam Interactions with Materials and Atoms* 259 (1): 7–13. https://doi.org/10.1016/j.nimb.2007.01.138.

Timar-Balazsy, Agnes, and Dinah Eastop. 2012. *Chemical Principles of Textile Conservation*. London: Routledge.

Watson, Andrew M. 1974. “The Arab Agricultural Revolution and Its Diffusion, 700–1100.” *The Journal of Economic History* 34 (1): 8–35. https://doi.org/10.1017/S0022050700079602.

———. 1983. *Agricultural Innovation in the Early Islamic World : The Diffusion of Crops and Farming Techniques, 700-1100 / Andrew M. Watson*. Cambridge: Cambridge university.